

A dynamical model of the adaptive immune system: effects of cells promiscuity, antigens and B-B interactions

Silvia Bartolucci¹ and Alessia Annibale^{1,2}

¹ Department of Mathematics, King's College London, The Strand, London WC2R 2LS, UK

² Institute for Mathematical and Molecular Biomedicine, King's College London, Hodgkin Building, London SE1 1UL, UK

Abstract. We analyse a minimal model for the primary response in the adaptive immune system comprising three different players: antigens, T and B cells. We assume B-T interactions to be diluted and sampled locally from heterogeneous degree distributions, which mimic B cells receptors' promiscuity. We derive dynamical equations for the order parameters quantifying the B cells activation and study the nature and stability of the stationary solutions using linear stability analysis and Monte Carlo simulations. The system's behaviour is studied in different scaling regimes of the number of B cells, dilution in the interactions and number of antigens. Our analysis shows that: (i) B cells activation depends on the number of receptors in such a way that cells with an insufficient number of triggered receptors cannot be activated; (ii) idiotypic (i.e. B-B) interactions enhance parallel activation of multiple clones, improving the system's ability to fight different pathogens in parallel; (iii) the higher the fraction of antigens within the host the harder is for the system to sustain parallel signalling to B cells, crucial for the homeostatic control of cell numbers.

Contents

1	Introduction	3
2	The model	4
2.1	Dynamical equations	6
3	Overview of results	9
4	Effects of receptors' promiscuity	10
4.1	A toy model with two B-clones	11
4.2	The case of P B clones with a variable number of receptors	15
4.2.1	Bifurcations near the critical temperature and stability region in the regime of competing clones.	16
4.2.2	Sequential B-clones activation: critical temperature and interference effects.	19
4.2.3	Numerical examples.	21
5	Idiotypic interactions	26
5.1	Dynamical equations for two B clones	27
5.2	Generalisation to P clones	30
5.2.1	Linear stability analysis and phase diagram	32
6	Antigen effect	34
7	Conclusions	38
8	Acknowledgements	39

1. Introduction

The immune system is a complex collection of organs, tissues and cells which is present in all vertebrates and protects the organism from external pathogens [1]. In this work we introduce a minimal model to describe the primary response of the adaptive immune system, a network of highly specialised cells that produces a targeted reaction to specific antigens, *i.e.* viruses. The main players are B and T cells, two different types of lymphocytes. They independently recognise the antigen binding it with their receptors (fig. 1). Each group of T and B cells sharing the same receptors' structure (clone) is able to recognise and fight *only* a particular virus with complementary epitope.

The immune response by B cells is activated or suppressed according to a confirmation signal sent by T cells in the form of excitatory or inhibitory proteins, the cytokines. Such response (when activated) consists in the secretion of antibodies, proteins able to chemically bind and neutralise the antigen, hence (possibly) avoiding the propagation of the infection. This two-signals mechanism prevents erroneous B cells activations against mismatching antigens or other cells of the organism.

In recent years, this system composed by a large number of interacting agents - T, B cells and antigens - has been looked at through the prism of statistical mechanics to understand its global features and functionalities [2, 3, 4, 5]. Following this promising line of research we propose here a model for the dynamics of T and B cells and antigens, extending preliminary proposals (see [5, 6] and references therein) to incorporate important biological features of real immune systems. In particular, we study the effect of having B cells with a variable number of receptors on their surfaces, one of the most important mechanisms preventing autoimmune reactions and diseases: a *receptor editing process* is indeed very commonly observed during the B cell maturation, where self-reactive cells, which may be responsible for the onset of autoimmune responses, are suppressed at an early stage of the development by changing the number of receptors [7]. We also introduce interactions between B cells, the so-called *idiotypic network*, first hypothesised by Jerne [8]: B cells receptors can not only recognise antigens but also other B cells with complementary receptors. In the presence of an antigen antibodies with complementary receptors, called *idiotypes* and denoted with Ab1, are produced and recognised by complementary antibodies (Ab2) which share structural features with the original antigen. According to recent experimental studies [9, 10, 11] the idiotypic network seems to play a central role in autoimmune diseases, supporting a cascade of autoantibodies production, which recognise each other and modulate the immune response. Finally, we incorporate the effect of an external antigenic field to investigate the *immunological memory* [12], *i.e.* the ability of the immune system to produce a more effective and faster response at a second encounter with an antigen.

From a statistical mechanics perspective this system is modelled as a bipartite network, where links between B and T-cells are sparse as biologically required. We introduce a phenomenological Hamiltonian description of the system and carry out a dynamical analysis of the network, evolving via a Glauber sequential update. Via non equilibrium statistical mechanical techniques initially

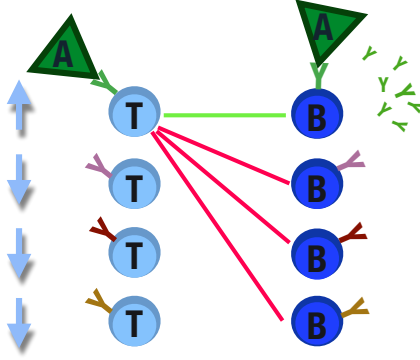


Figure 1. Schematic representation of the antigen recognition process and immune response activation by T and B cells. The best-matching B and T cells independently detect the antigen: the active T clone sends excitatory cytokines (green links) to the B clone to start the antibodies production and suppress the non-complementary B clones with inhibitory signals (red). The other T cells are in a quiescent state.

developed for Hopfield neural networks and spin glasses [13, 14, 15, 16, 17] we derive the equations for the time evolution of a set of parameters, quantifying the immune response strength. We analyse the system’s behaviour in different regions of the parameter’s space (*i.e.* number of clones and triggered receptors, noise level, *etc.*) through linear stability analysis and Monte Carlo simulations. The paper is structured as follows: in Sec. 2 we define the model, in Sec. 3 we give an overview of the results that we derive in Sec. 4, 5 and 6. We summarise our conclusions in 7.

2. The model

We model T-cells as binary variables or “spins” $\sigma_i = \pm 1$, $i = 1, \dots, N$, which can be active *i.e.* secreting cytokines (+1) or quiescent (−1). B cells and antigens are characterised via their concentration, respectively $b_\mu \in \mathbb{R}$, $\mu = 1, \dots, P$ and $\psi_a \in \mathbb{R}$, $a = 1, \dots, A$ with respect to a reference level. Both the number of B clones and the number of antigens are sub-linear in the system size N , with $P = N^\delta$, $\delta \in [0, 1)$ and $A = N^a$, $a \in [0, 1)$. In the absence of antigens and interactions with T cells, the B clone sizes b_μ can be regarded as Gaussian variables [12]. Without loss of generality we take their mean to be zero and we denote by \mathbf{A}^{-1} their covariance matrix.

The interactions between the i -th T clone and the μ -th B clone, mediated via the cytokines, are represented by the variables $\xi_i^\mu \in \{+1, -1, 0\}$, respectively corresponding to excitatory, inhibitory or absent signals. We will regard those as random variables drawn from

$$P(\boldsymbol{\xi}) = \prod_{i\mu} \left[\frac{q_\mu}{2N^\gamma} (\delta_{\xi_i^\mu, 1} + \delta_{\xi_i^\mu, -1}) + \left(1 - \frac{q_\mu}{N^\gamma} \right) \delta_{\xi_i^\mu, 0} \right], \quad q^\mu = \mathcal{O}(N^0) \quad \forall \mu, \quad (1)$$

where the q_μ ’s are drawn from a distribution $\mathcal{P}(q) = P^{-1} \sum_\mu \delta_{q, q_\mu}$ and control the degree of B cells promiscuity, *i.e.* their ability to communicate with different T cells, via different receptors.

The fraction of non-zero B-T links determines the degree of dilution of the system: for $\gamma = 0$ the system is finitely diluted, whereas for $\gamma > 0$ the system is extremely diluted. The combined interacting system of B-T cells and the antigens can be phenomenologically described by the following Hamiltonian:

$$\mathcal{H}(\boldsymbol{\sigma}, \mathbf{b}) = - \sum_{\mu=1}^P b_{\mu} \left(\sum_{a=1}^A \psi_a \eta_a^{\mu} + N^{1-\gamma} \sum_{i=1}^N \xi_i^{\mu} \sigma_i \right) + \frac{1}{2\sqrt{\beta}} \sum_{\nu,\mu=1}^P b_{\mu} A_{\mu\nu} b_{\nu}. \quad (2)$$

The first term takes into account the interactions between antigens and B cells via the matrix η_a^{μ} , the second term is related to B - T interactions mediated by cytokines, the third one takes into account the effect of the idiotypic network (B-B interactions) (fig. 2). B-B interactions are mediated via $\mathbf{A} = \{A_{\mu\nu}\}$: according to the theory of idiotypic interactions [8, 20], B clones can recognise not only antigens but also antibodies with complementary epitopes creating a network of imitative interactions between B cells. We represent epitopes as binary strings and assume that complementary strings, like e.g. 010... and 101..., excite each other. Also, we assume that we can order the strings on a ring in such a way that each string sits close to affine strings and opposite to complementary ones (fig. 3, right). Hence, we suppose that the μ -th B clone expansion is triggered by the $(\mu + P/2)$ -th B clone, which is precisely complementary to that B clone (fig. 3, left). While complementary B cells excite each other, we assume that each B cell suppresses itself, to prevent uncontrolled production of a single cell type. Therefore, we are led to use for the B-B interactions the Toeplitz matrix

$$A_{\mu\nu} = \delta_{\mu\nu} - k \delta_{\mu,(\nu+P/2) \bmod P}, \quad (3)$$

with $k \in [0, 1)$ representing the strength of idiotypic interactions. Its inverse is

$$(A^{-1})_{\mu\nu} = \frac{1}{1-k^2} \delta_{\mu\nu} + \frac{k}{1-k^2} \delta_{\mu,(\nu+P/2) \bmod P}. \quad (4)$$

We note that \mathbf{A} is positive definite and symmetric and the following relations hold: $A_{\mu\nu} = A(\mu-\nu)$ with $A(n+P) = A(n)$ and $A(n) = A(-n)$. The eigenvalue spectrum $\rho(a)$ of \mathbf{A} has a finite limit as $N \rightarrow \infty$, ensuring the correct scaling of the Hamiltonian. B-antigen interactions are taken into account via the matrix η_a^{μ} : antigens will excite complementary B and they will repress the identical one, in a similar way as B clones detect and excite each other as shown in fig. 4. We can further investigate the B-Antigen interactions analysing the stochastic process that governs the dynamics of B cells concentration. Assuming that the B cells concentration evolves according to a gradient descent on the Hamiltonian (2), we have

$$\frac{db_{\mu}}{dt} = - \frac{\partial \mathcal{H}}{\partial b_{\mu}} + noise = \sum_{a=1}^A \psi_a \eta_a^{\mu} + N^{\gamma-1} \sum_{i=1}^N \xi_i^{\mu} \sigma_i - \frac{1}{2\sqrt{\beta}} \sum_{\nu=1}^P A_{\mu\nu} b_{\nu} + noise. \quad (5)$$

Denoting with ψ_{μ} the concentration of the antigen complementary to the b_{μ} clone, we need the b_{μ} concentration to increase when $\psi_{\mu} \neq 0$. Also, we assume that clone $b_{\mu+p/2}$, complementary to b_{μ} and thus carrying the same epitope as antigen ψ_{μ} , is inhibited by the presence of antigen ψ_{μ} , and we denote k_1 the strength of this inhibition. This leads to a matrix for the B-Antigen interaction

in the form

$$\eta_a^\mu = \delta_{\mu a} - k_1 \delta_{\mu, (a+P/2) \bmod P} \quad (6)$$

According to (5), the concentration of the μ -th clone also increases in the presence of excitatory signals received by T cells (second term) while the third suppressive term is related to B-B interactions acting as a threshold to be overcome to start the immune response. Assuming that the total B clones concentration is conserved on average leads to a relation between k and k_1

$$\frac{d}{dt} \sum_\mu b_\mu = 0 \rightarrow \frac{1 - k_1}{1 - k} = \frac{1}{2\sqrt{\beta}} \frac{\sum_\nu b_\nu}{\sum_a \psi_a} \quad (7)$$

which depends on the steady state concentrations of B cells and antigens and on the inverse noise level $\sqrt{\beta}$. For simplicity we will set $k = k_1$, which leads to $\boldsymbol{\eta} = \mathbf{A}$ and to an equilibrium ratio between B cells and antigens concentration only controlled by the noise level in the system.

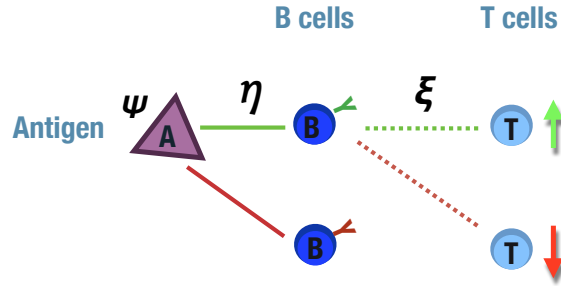


Figure 2. Schematic interactions between B, T cells and the antigen A. In the presence of an antigen with concentration ψ , the complementary B cell will detect it (B-A interactions mediated via the matrix $\boldsymbol{\eta}$) and will receive a confirmatory signal from the active T cells (represented by up arrows) via the cytokines ξ_i^μ .

2.1. Dynamical equations

At equilibrium at inverse noise level $\sqrt{\beta}$, (consistent with our assumption $\mathbf{b} \sim \mathcal{N}(0, \mathbf{A}^{-1})$) we expect the joint distribution $P(\boldsymbol{\sigma}, \mathbf{b})$ to be given by the Boltzmann distribution

$$P(\boldsymbol{\sigma}, \mathbf{b}) = \frac{e^{-\sqrt{\beta}\mathcal{H}(\boldsymbol{\sigma}, \mathbf{b})}}{Z} \quad (8)$$

The equilibrium marginal distribution for the $\boldsymbol{\sigma}$ is found, by integrating out the variables b_μ ,

$$\begin{aligned} P(\boldsymbol{\sigma}) &= \frac{1}{Z} \int d\mathbf{b} e^{\sqrt{\beta} [\sum_\mu b_\mu (\sum_a \psi_a \eta_a^\mu + N^{\gamma-1} \sum_i \xi_i^\mu \sigma_i) - \frac{1}{2} \sum_{\nu, \mu} b_\mu A_{\mu\nu} b_\nu]} \\ &= \frac{1}{Z'} e^{\beta \left[\frac{N^2(\gamma-1)}{2} \sum_{ij} \sigma_i \sigma_j \sum_{\mu, \nu} \xi_i^\mu (A^{-1})_{\mu\nu} \xi_j^\nu + N^{\gamma-1} \sum_{ia} \sigma_i \psi_a \sum_{\mu, \nu} \eta_a^\mu (A^{-1})_{\mu\nu} \xi_i^\nu \right]}, \end{aligned} \quad (9)$$

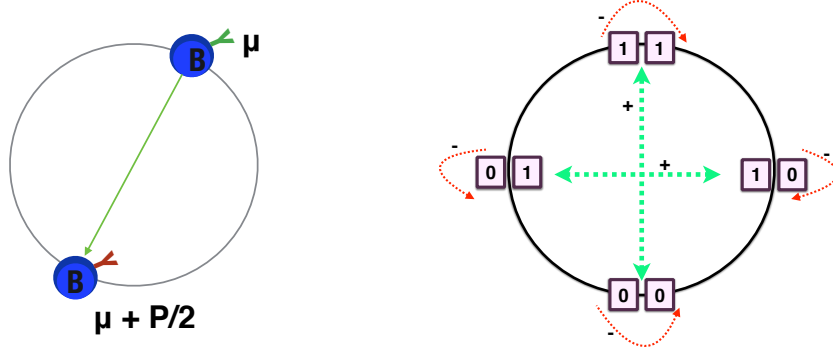


Figure 3. Left: B-B interaction via $A_{\mu\nu}$. The expansion of the μ -th clone is triggered by its complementary clone. Right: We represent the epitopes as binary strings, organising them on a ring and assuming that the complementary strings interact.

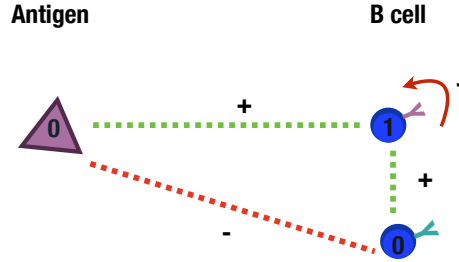


Figure 4. Scheme of B-B and B-A interactions. Antigens and B cells are denoted by variables 0,1 representing the shape of their receptors: 0 – 1 variables represent complementary receptors (key-lock mechanism). Different B cells excite each other and each of them represses itself, while the antigen will excite complementary B repressing the identical one (0-0).

in the Boltzmann form with effective Hamiltonian $\mathcal{H}(\boldsymbol{\sigma})$, involving only interactions between T cells,

$$\mathcal{H}(\boldsymbol{\sigma}) = -\frac{1}{2}N^{2(\gamma-1)} \sum_{ij} \sigma_i \sigma_j \sum_{\mu,\nu} \xi_i^\mu (A^{-1})_{\mu\nu} \xi_j^\nu + N^{\gamma-1} \sum_{ia} \sigma_i \psi^a \sum_{\mu,\nu} \eta_a^\mu (A^{-1})_{\mu\nu} \xi_i^\nu \quad (10)$$

with the separable form $J_{ij} = N^{2(\gamma-1)} \boldsymbol{\xi}_i \mathbf{A}^{-1} \boldsymbol{\xi}_j$, where $\boldsymbol{\xi}_i = (\xi_i^1, \dots, \xi_i^P)$, and thus describing an associative network with diluted patterns $\{\boldsymbol{\xi}^\mu\}$, encoding fighting strategies against different antigens [6]. In the regime we consider here $\delta < 1$, the associative network is away from saturation. Analysis near saturation have been carried out in statics for $\mathbf{A} = \mathbf{1}$, mostly for $\mathcal{P}(q) = \delta(q - c)$ [18, 19]. We can rewrite the Hamiltonian (10) as

$$\mathcal{H}(\boldsymbol{\sigma}) = -\frac{1}{2} \mathbf{M}^T(\boldsymbol{\sigma}) \mathbf{A}^{-1} \mathbf{M}(\boldsymbol{\sigma}) + \boldsymbol{\psi}^T \boldsymbol{\eta} \mathbf{A}^{-1} \mathbf{M}(\boldsymbol{\sigma}) \quad (11)$$

in terms of the order parameters $\mathbf{M} = (M_1, \dots, M_P)$, where

$$M_\mu(\boldsymbol{\sigma}) = \frac{1}{N^{1-\gamma}} \sum_{i=1}^N \sigma_i \xi_i^\mu \quad (12)$$

quantifies the strength of the excitatory signal on B clone μ and thus its activation. Here $\boldsymbol{\psi} = (\psi_1, \dots, \psi_P)$ and we denote \mathbf{v}^T the transpose of \mathbf{v} . Next, we assume a Glauber sequential dynamics for the variables $\boldsymbol{\sigma}$, converging to the equilibrium measure $P(\boldsymbol{\sigma})$, so that the instantaneous probability of finding the system in state $\boldsymbol{\sigma} = (\sigma_1, \dots, \sigma_N)$ at time t is governed by the master equation

$$\frac{\partial P_t(\boldsymbol{\sigma})}{\partial t} = \sum_{i=1}^N [P_t(F_i \boldsymbol{\sigma}) w_i(F_i \boldsymbol{\sigma}) - P_t(\boldsymbol{\sigma}) w_i(\boldsymbol{\sigma})], \quad (13)$$

where F_i is the i -th spin-flip operator $F_i(\sigma_1, \dots, \sigma_i, \dots, \sigma_N) = (\sigma_1, \dots, -\sigma_i, \dots, \sigma_N)$ and transition rates between $\boldsymbol{\sigma}$ and $F_i \boldsymbol{\sigma}$ have the Glauber form

$$w_i(\boldsymbol{\sigma}) = \frac{1}{2} [1 - \sigma_i \tanh(\beta h_i^{\text{eff}}(\boldsymbol{\sigma}))], \quad (14)$$

with effective field

$$h_i^{\text{eff}} = N^{\gamma-1} (\mathbf{M}^T \mathbf{A}^{-1} \boldsymbol{\xi}_i + \boldsymbol{\psi}^T \boldsymbol{\eta} \mathbf{A}^{-1} \boldsymbol{\xi}_i) \quad (15)$$

ensuring convergence to (9). Here $T = 1/\beta$ represents the rate of spontaneous spin-flip, hence the effective noise of the T cell dynamics. Using (13), we write the dynamics for the B cells activation, described by the probability of finding the system in a macroscopic state \mathbf{M} at time t , namely

$$P_t(\mathbf{M}) = \sum_{\boldsymbol{\sigma}} P_t(\boldsymbol{\sigma}) \delta(\mathbf{M} - \mathbf{M}(\boldsymbol{\sigma})). \quad (16)$$

Via a Kramers-Moyal expansion for large system size and away from the saturation regime it is possible to show that $P_t(\mathbf{M})$ evolves according to a Liouville equation [6]. It follows that \mathbf{M} evolve deterministically with a dynamics described by

$$\frac{d\mathbf{M}}{dt} = \left\langle \boldsymbol{\xi}^T \tanh [\beta (\mathbf{M}^T \mathbf{A}^{-1} \boldsymbol{\xi} + \boldsymbol{\psi}^T \mathbf{C} \boldsymbol{\xi})] \right\rangle_{\boldsymbol{\xi}} - \mathbf{M} \quad (17)$$

where $\mathbf{C} = \boldsymbol{\eta} \mathbf{A}^{-1}$ and $\langle \cdot \rangle_{\boldsymbol{\xi}}$ denotes the average over the distribution (1). For $\boldsymbol{\eta}$ defined in (6) and $k = k_1$, we have $\mathbf{C} = \mathbf{1}$, and each order parameter M_μ evolves according

$$\frac{dM_\mu}{dt} = \left\langle \xi^\mu \tanh \left[\beta (\mathbf{M}^T \mathbf{A}^{-1} \boldsymbol{\xi} + \boldsymbol{\psi}^T \boldsymbol{\xi}) \right] \right\rangle_{\boldsymbol{\xi}} - M_\mu. \quad (18)$$

Different choices of the matrix $\boldsymbol{\eta}$ or of the constants k, k_1 will lead to different forms of the matrix \mathbf{C} , however the choice $\mathbf{C} = \mathbf{1}$ seems to ensure the strongest excitatory signal to antigen-activated B clones. As an illustration, let us consider the simple case where we have just one antigen *i.e.* ψ_1 : for the choice $\mathbf{C} = \mathbf{1}$ the field acting on the i -th T cell exciting the complementary clone b_1 is ψ_1 , hence i receives an activation signal only from the clone B activated by the antigen. With two antigens present, whose complementary B cells are signalled by different cytokines from the same

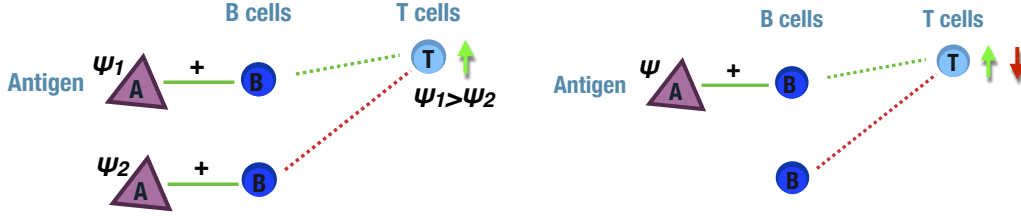


Figure 5. Left: effect of having $\mathbf{C} = \mathbf{1}$, in the presence of two antigens whose complementary B cells are signalled by different cytokines from the same T cell: the field acting on the T cell is $\psi_1 - \psi_2$ and T gets activated only if $\psi_1 > \psi_2$. Right: an illustration of the effect of having $\mathbf{C} = \mathbf{A}^{-1}$, which may result in an inhibitory signal on T cells from inactive B cells.

T cell, the field acting on the latter is $\psi_1 - \psi_2$ and the T cell will get activated only if $\psi_1 > \psi_2$, as biologically desired (fig. 5, left). For $\mathbf{C} \neq \mathbf{1}$ there might be a negative interference on the desired signal. For example, for the alternative choice $\boldsymbol{\eta} = \mathbf{1}$, leading to $\mathbf{C} = \mathbf{A}^{-1}$, the field acting on T in the presence of a single virus $\psi_1 \neq 0$ would be $\frac{\psi_1}{1-k^2} [\xi_i^1 + k\xi^{1+\frac{P}{2}}]$, meaning that for $\xi^1 = +1$, $\xi^{1+\frac{P}{2}} = -1$ the T cell would receive, besides the excitatory signal from the B cell activated by the antigen, an inhibitory signal from a non-activated B-cell (fig. 5, right). As a result the overall field and immune response will decrease. Similar arguments can be given for $\boldsymbol{\eta}$ defined in (6) with $k_1 \neq k$.

3. Overview of results

The sparsity of the B-T connections makes the system able to activate multiple B clones in parallel. This multitasking capability is one of the core features of the immune system that, in normal conditions, can control and block several simultaneous antigenic invasions. We find that the parallel activation of B clones may occur in *symmetric* fashion, where all infections are fought with the same strength, or in a *hierarchical* fashion, where the system prioritises immune responses against specific pathogens. We are able to identify the system's parameters, such as noise, number of links, number of different infections, which induce the switch from the symmetric to the hierarchical operational mode. This might be potentially useful to investigate the causes of dramatic failures in the functioning of the immune system. The switch to a hierarchical immune response is in fact mostly related to the presence of strong infections, such as hepatitis and autoimmune disorders: while the immune system invests the highest amount of resources tackling the main disease, the progression of minor infections may become lethal [21, 22].

An important feature of the model is the dependence of the B cells activation on the number of receptors on their surface. Results in Sec. 4 show that cells with few receptors may be transiently activated but fail to sustain the signal even if strongly excitatory (fig. 6). The number of triggered receptors affects both the immune response strength and the critical temperature at which they get activated: both decrease with the number of triggered receptors. In addition, competition

emerges between B clones to be activated. As the number of activated B clones increases, signalling pathways to inactive clones get more noisy due to the interference of active clones. The critical temperature for the activation of inactive clones is a decreasing function of the fraction of active clones (73).

Another result of biological interest is that idiotypic *i.e.* B-B interactions contribute to the overall stability of the immune system, preventing unwanted activation and increasing the region where all clones are equally activated and ready to start an immune response upon arrival of new infections (Sec. 5). In particular, including B-B interactions in the model affects the critical temperature, in this case widening the region where a symmetric immune response is stable, as the interactions strength k is increased (fig. 22).

Finally, the role of antigens in B cells activation is understood by our model as that of external fields on coupled ferromagnetic systems 6. One of the interesting consequences is then the presence of hysteresis phenomena [23], which could explain short-term memory effect in the immune response [12, 24], even in the absence of memory cells. The effect of antigens on the immune system *basal activity* and surveillance is also of interest: the response of non-infected B clones decreases with the fraction of infected clones, due to the interference of strongly activated B cells, and is activated at a lower T , making the whole system unresponsive to new incoming viruses (fig. 23).

4. Effects of receptors' promiscuity

We first consider the case where there is no antigen $\psi_a = 0 \forall a$, and no B-B interactions *i.e.* $\mathbf{A} = \mathbf{1}$ and focus on the effect of having a variable number of triggered receptors on different B clones, *i.e.* heterogeneous q_μ in (1). In order to compare activation of B clones with different numbers of receptors, it is convenient to look at the activation per receptor, given by the normalised order parameters $m_\mu = M_\mu/q_\mu$, $\mu = 1, \dots, P$, which take values in the range $[-1, 1]$ for all clones μ . The dynamical equations (18) then read

$$\frac{dm_\mu}{dt} = \frac{N^\gamma}{q_\mu} \left\langle \xi_\mu \tanh \left(\beta \sum_\nu q_\nu \xi^\nu m_\nu \right) \right\rangle_\xi - m_\mu . \quad (19)$$

One can show that at the critical temperature $T_c = q_{\max}$, where $q_{\max} = \max_\mu [q_\mu]$, the system undergoes a phase transition, with the equilibrium phase at $T > T_c$ characterised by $\mathbf{m} = \mathbf{0}$, and B clones activation occurring at $T < T_c$, where $\mathbf{m} \neq \mathbf{0}$. At the steady state ($d\mathbf{m}/dt = 0$), we have

$$M_\mu = N^\gamma \langle \xi^\mu \tanh(\beta \sum_\nu \xi^\nu M_\nu) \rangle_\xi . \quad (20)$$

Taking the scalar product with \mathbf{M} and using the inequality $|\tanh x| \leq |x|$, yields

$$\mathbf{M}^2 \leq N^\gamma \beta \sum_\mu M_\mu \sum_\nu M_\nu \langle \xi^\nu \xi^\mu \rangle_\xi = \beta \sum_\mu q_\mu M_\mu^2 \leq \beta q_{\max} \mathbf{M}^2 . \quad (21)$$

This implies $\mathbf{M}^2 = 0$, hence $\mathbf{m} = \mathbf{0}$, for $\beta q_{\max} < 1$, meaning that none of the B cells can get activated for noise levels above the critical value $T > q_{\max}$. Although $\mathbf{m} = \mathbf{0}$ is a steady state

solution of (19) for any value of T , a linear stability analysis shows that it becomes unstable for $T < q_{\max}$. To this purpose, we compute the Jacobian of the linearised dynamics about the steady state $\mathbf{m}^* = \mathbf{0}$

$$J_{\mu\nu} = \left. \frac{\partial F_{\mu}^{(1)}(\mathbf{m})}{\partial m_{\nu}} \right|_{\mathbf{m}=\mathbf{m}^*}, \quad F_{\mu}^{(1)}(\mathbf{m}) = \frac{N^{\gamma}}{q^{\mu}} \langle \xi^{\mu} \tanh(\beta \sum_{\nu=1}^P \xi^{\nu} q^{\nu} m_{\nu}) \rangle_{\xi} - m_{\mu} \quad (22)$$

which gives

$$J_{\mu\nu} = \frac{N^{\gamma} \beta q_{\nu}}{q_{\mu}} \langle \xi^{\nu} \xi^{\mu} [1 - \tanh^2(\beta \sum_{\nu} \xi^{\nu} q_{\nu} m_{\nu}^*)] \rangle_{\xi} - \delta_{\mu\nu}. \quad (23)$$

Substituting $\mathbf{m}^* = \mathbf{0}$ we get $J_{\mu\nu} = (\beta q_{\mu} - 1) \delta_{\mu\nu}$. This is a diagonal matrix, hence the largest eigenvalue, which gives the stability of $\mathbf{m}^* = 0$, is $\lambda_{\max} = \beta q_{\max} - 1$. This gets positive for $\beta q_{\max} > 1$, showing that non-zero solutions $\mathbf{m} \neq 0$ will bifurcate away from $\mathbf{m} = 0$ at $T = q_{\max}$. We inspect the structure and the stability of the bifurcating solutions first for a toy model with just two B-clones and then for the general case with P B-clones.

4.1. A toy model with two B-clones

Here we study a toy model with $P = 2$ B clones, and assume $q_1 > q_2$. For $\gamma > 0$ this model reduces to two independent Curie-Weiss ferromagnets, with critical temperatures q_1 and q_2 respectively (see discussion in Sec. 4.2). Hence, the most interesting case is obtained for $\gamma = 0$. The state $\mathbf{m}^* = (0, 0)$ is the only steady state of the system for $T > q_1$, but it destabilises for $T < q_1$. We can understand the system's behaviour below criticality by solving numerically its dynamical equations

$$\frac{dm_1}{dt} = (1 - q_2) \tanh(\beta q_1 m_1) + \frac{q_2}{2} [\tanh(\beta(q_1 m_1 + q_2 m_2)) + \tanh(\beta(q_1 m_1 - q_2 m_2))] - m_1, \quad (24)$$

$$\frac{dm_2}{dt} = (1 - q_1) \tanh(\beta m_2) + \frac{q_1}{2} [\tanh(\beta(q_1 m_1 + q_2 m_2)) - \tanh(\beta(q_1 m_1 - q_2 m_2))] - m_2. \quad (25)$$

In fig. 6 we show the flow diagram and the stable fixed points at different temperatures: first we notice that B cells with a higher promiscuity produce a higher immune response (m_1), whereas a lower promiscuity q_{μ} results in a lower or null activation (m_2) depending on the temperature. Hence, the number of receptors on B cells' surface affects the responsiveness of B clones. In particular, if T is high, only clones with the highest number of receptors are activated and the system's fixed point corresponds to the pure state $m_1 \neq 0, m_2 = 0$. Lowering T induces the activation of cells with fewer receptors but with a lower intensity ($m_1 > m_2$). Theoretical results are consistent with Monte Carlo simulations, shown in fig. 7. Furthermore, Monte Carlo simulations match experimental results [25] showing that cells with very few receptors are triggered transiently but fail to be activated in the long run, since the number of receptors is not sufficient to allow these cells to sustain the signal, even if strongly excitatory. Fig. 8 shows that our model can reproduce this effect: cells with few receptors (green) have a lower activation even if triggered by a strong signal (initial condition) and tends to be switched off after a short transient, conversely

cells with a higher number of receptors (blue) produce a strong immune response, even if triggered by a low signal (initial condition). Analytically, we can investigate the structure of the first states

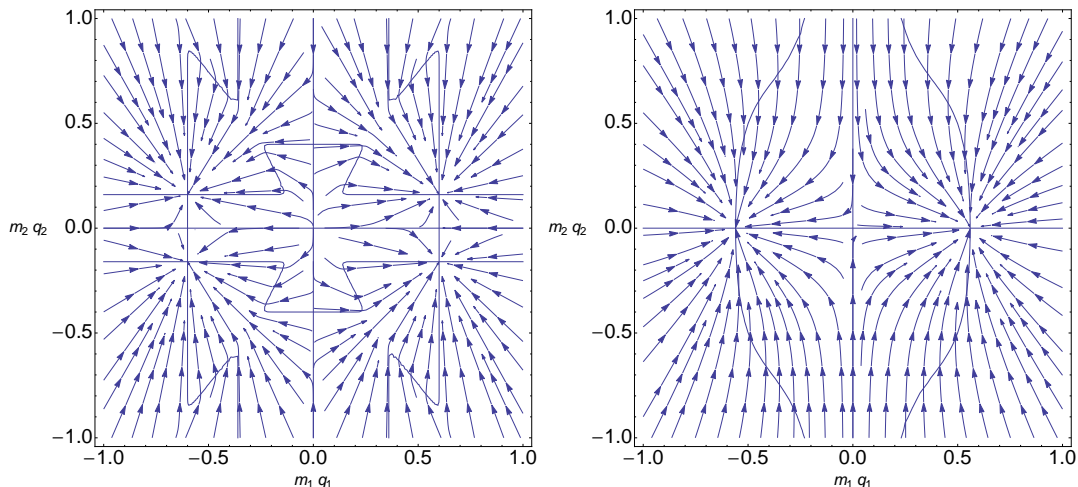


Figure 6. Phase portrait of the dynamical system (24, 25) for $q_1 = 0.6$, $q_2 = 0.4$ at low temperature $T = 0.01$ (left) and high temperature $T = 0.2$ (right). Red lines represent null-clines and stationary states are at the intersection of null-clines.

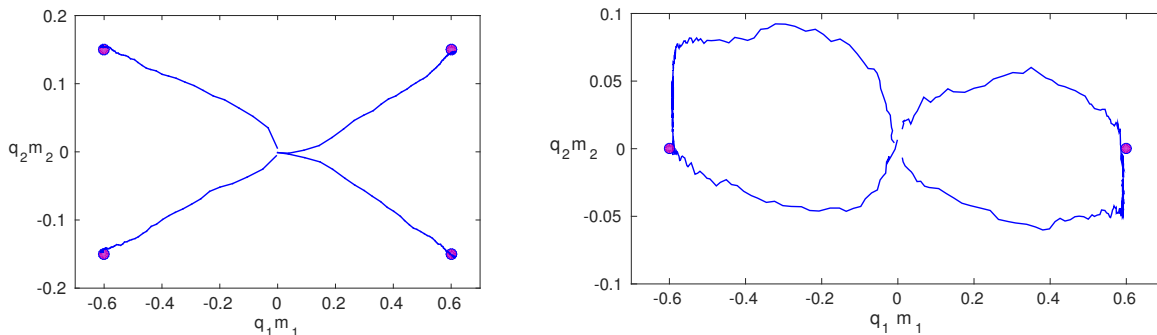


Figure 7. Monte Carlo simulations with 10^4 spins for $q_1 = 0.6$, $q_2 = 0.4$ at low temperature $T = 0.01$ (left) and at high temperature $T = 0.2$ (right). Markers represent the numerical solutions of (24, 25).

to bifurcate below T_c by expanding the steady state equations, obtained setting $dm_{1,2}/dt = 0$ in (24, 25), for small m_1, m_2 , close to criticality, *i.e.* at $\beta q_1 = 1 + \epsilon$. We get as possible solutions

$$m_1^2 = 3\epsilon - 3\frac{q_2^3}{q_1^2}m_2^2, \quad (26)$$

$$m_2^2 = 3\frac{q_1^2}{q_2^2}(1 + \epsilon) - 3\frac{q_1^3}{q_2^3} - 3\frac{q_1^3}{q_2^2}m_1^2, \quad (27)$$

as well as $m_1 = 0, m_2 = 0$. Solution (27) is unphysical as it stays $\mathcal{O}(1)$ at $\epsilon = 0$ for $q_1 \neq q_2$, hence $m_2 = 0$. Inserting $m_2 = 0$ in (26), we get $m_1^2 = 3\epsilon$. Hence, the first state bifurcating away from

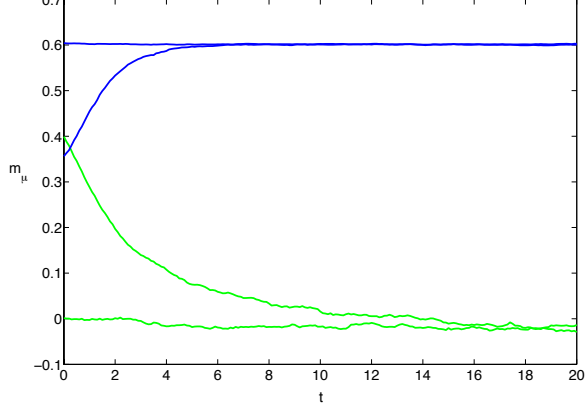


Figure 8. Monte Carlo simulations with $N = 10^4$ spins, with $q_1 = 0.6$, $q_2 = 0.4$ at $T = 0.2$. Clone activation m_1 , m_2 as a function of time for different initial conditions. Cells with few receptors, q_2 (green) fail to be activated even if triggered with a strong signal.

$\mathbf{m} = (0, 0)$ is in the form $\mathbf{m} = (\sqrt{3\epsilon}, 0)$. At high temperature (below criticality) only the clone with the higher number of receptors is switched on. For $q_1 = q_2$ we clearly retrieve the results in [6] and both B clones are activated with the same intensity below criticality. Next we derive the region in the phase diagram where cells with fewer receptors become responsive. Naively one might expect that m_2 becomes active at $T \simeq q_2$. In reality, heterogeneities in the cell promiscuities deeply affects cell responsiveness and cells with fewer receptors will remain quiescent even at very low T . By Taylor expanding (19) for small m_2 in powers of $\epsilon = q_2\beta - 1$, we obtain

$$m_1 = \tanh(\beta q_1 m_1) \simeq \tanh\left(\frac{q_1}{q_2} m_1\right), \quad (28)$$

$$m_2^2 = 3\epsilon - 3\frac{q_1^3}{q_2^2} m_1^2. \quad (29)$$

Since m_1 is $\mathcal{O}(1)$ the non-zero solution for m_2 is impossible close to $T = q_2$. The pure state $\mathbf{m} = (m_1, 0)$ will then have a wider stability region, that can be found by analysing the eigenvalues of the Jacobian (22) at $\mathbf{m}^* = (m_1, 0)$,

$$\lambda_1 = \beta q_1 - \beta q_1 \tanh^2(\beta q_1 m_1) - 1, \quad (30)$$

$$\lambda_2 = \beta q_2 - \beta q_1 q_2 \tanh^2(\beta q_1 m_1) - 1. \quad (31)$$

Analytically we can calculate $\lambda_{1,2}$ near $T \simeq 0$

$$\lambda_1 \simeq -1, \quad (32)$$

$$\lambda_2 \simeq \beta q_2 - \beta q_1 q_2 - 1. \quad (33)$$

and near T_c , *i.e.* at $\beta q_1 = 1 + \epsilon$

$$\lambda_1 \simeq -2\epsilon, \quad (34)$$

$$\lambda_2 \simeq \frac{q_2\epsilon + q_2 - 3\epsilon q_1 q_2 - q_1}{q_1} + \mathcal{O}(\epsilon^2). \quad (35)$$

For intermediate T we compute $\lambda_{1,2}$ numerically. Plots of eigenvalues as a function of the

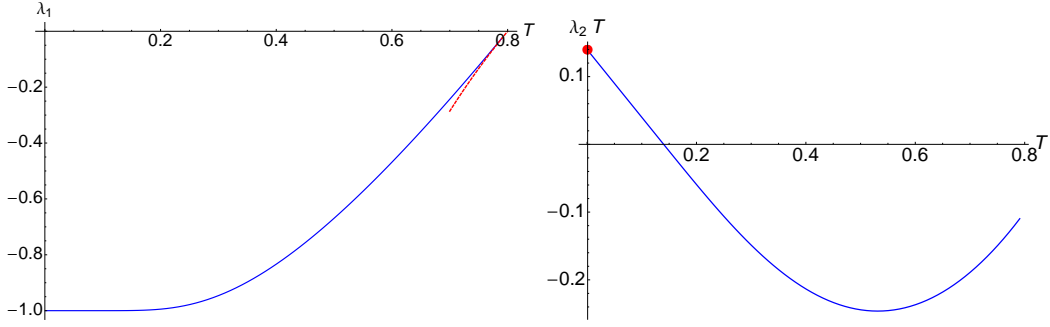


Figure 9. Eigenvalues (31) as a function of T for $q_1 = 0.8$ and $q_2 = 0.7$. Left: λ_1 , the red dashed line represents the behaviour near $T \simeq T_c$ (35). Right: $\lambda_2 T$, the red marker represents the limit at $T \simeq 0$ (33).

temperature are shown in fig. 9 where the theoretical predictions for $T \simeq 0$ (33) and $T \simeq T_c$ (35) are highlighted. We note that $\lambda_1 < 0, \forall T$, hence the stability of the pure state is determined by the sign of λ_2 . In fig. 10 we show a contour plot of $\lambda_2 = 0$ in the $T - q_2$ plane for different values of q_1 . The linear behaviour can be understood as follows. In the pure state region we have,

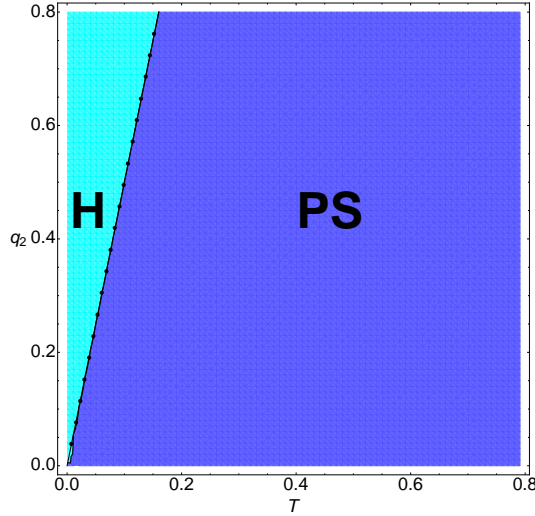


Figure 10. Phase diagram in the space (T, q_2) fixing $q_1 = 0.8$ obtained from the condition $\lambda_2 < 0$ (31). The dotted line represents the theoretical critical temperature (38). In the **(PS)** region the pure state is stable ($m_1 \neq 0, m_2 = 0$). At low T , B clones are hierarchically activated (**H**).

using the steady state equation $m_1 = \tanh(\beta q_1 m_1)$,

$$\lambda_1 = \beta q_1 (1 - m_1^2) - 1, \quad (36)$$

$$\lambda_2 = \beta q_2 (1 - q_1 m_1^2) - 1. \quad (37)$$

As T decreases (below q_2) m_1 increases, so that the eigenvalues stay negative and stability is ensured, until m_1 reaches its maximum value $m_1 = 1$. At this point, a further decrease of the

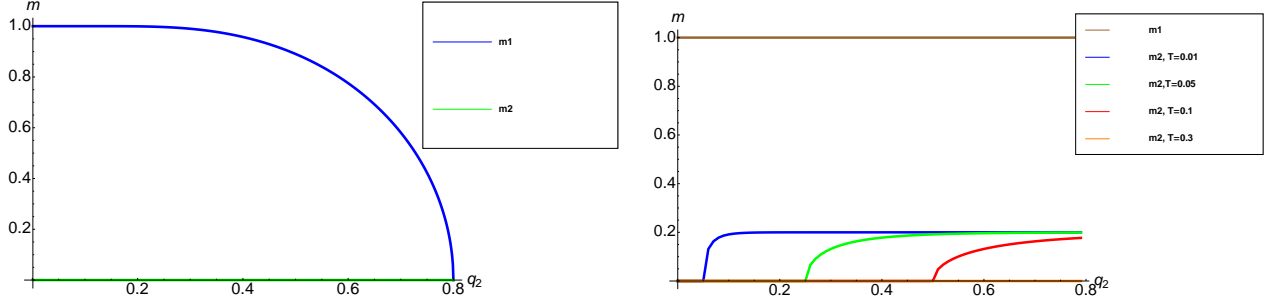


Figure 11. Plot of m_1, m_2 as a function of q_2 . Left : $q_1 = 0.8$ at $T = q_2$, Right: $q_1 = 0.8$, $T = 0.01, 0.05, 0.1, 0.3$.

temperature will make λ_2 positive, destabilising the pure state, and a new state (m_1, m_2) will take over. The temperature at which bifurcations from the pure state are expected is thus found from the condition $\lambda_2(T, m_1 = 1) = 0$, as

$$T = q_2(1 - q_1) \quad (38)$$

which is in agreement with the critical temperature computed numerically (fig. 10). Deviations from the linear behaviour are expected in the regime $q_1 \simeq q_2$, where a symmetric activation occurs for $q_1 \leq 1/3$ [6]. In fig. 11 we plot m_1, m_2 as a function of q_2 in the **(PS)** region (left) and crossing the critical line where m_2 becomes non-zero (right). In the latter region, *i.e.* for $q_2 > T/(1 - q_1)$, the stable state is $\mathbf{m} = (1, m_2)$ where m_2 is the T -dependent stationary solution of (25) at $m_1 = 1$. In particular, for $T = 0$ the stable state is

$$m_1 = 1, \quad (39)$$

$$m_2 = 1 - q_1, \quad (40)$$

in agreement with simulations and flow diagrams (fig. 6, 7). In conclusion, the system can activate clones with different numbers of receptors simultaneously for $T < q_2(1 - q_1)$. The activation is hierarchical (**H**), with clones with higher promiscuity being prioritised with respect to the others. In particular, clones with the highest number of receptors are activated with the strongest possible signal in a wide region of the phase diagram.

4.2. The case of P B clones with a variable number of receptors

Next we study the case where the number of B clones is $P = N^\delta$ where $\delta \in [0, 1)$, and N is the number of T-clones. The dynamical equations are

$$\frac{dm_\mu}{dt} = \frac{N^\gamma}{q_\mu} \left\langle \xi_\mu \tanh \left(\beta \sum_\nu q^\nu \xi^\nu m_\nu \right) \right\rangle_\xi - m_\mu, \quad (41)$$

which can be rewritten as

$$\frac{dm_\mu}{dt} = \left\langle \tanh \left(\beta (q^\mu m_\mu + \sum_{\nu \neq \mu} q^\nu \xi^\nu m_\nu) \right) \right\rangle_{\xi_\mu \neq 0} - m_\mu. \quad (42)$$

Upon introducing the noise distribution $P_\mu(z|\{m_\nu, q_\nu\}) = \langle \delta(z - \sum_{\nu \neq \mu} \xi^\nu q_\nu m_\nu) \rangle_{\boldsymbol{\xi}}$ on clone μ , we have

$$\frac{dm_\mu}{dt} = \int dz P_\mu(z|\{m_\nu\}) \tanh(\beta(q_\mu m_\mu + z)) - m_\mu \quad (43)$$

where $P_\mu(z|\{m_\nu, q_\nu\})$ can be written, using the Fourier representation of the Dirac delta and carrying out the average over $\boldsymbol{\xi}$, as

$$P_\mu(z|\{m_\nu, q_\nu\}) = \int_{-\infty}^{+\infty} \frac{d\omega}{2\pi} e^{iz\omega} \langle \prod_{\nu \neq \mu}^P e^{-i\omega \xi^\nu q_\nu m_\nu} \rangle_{\boldsymbol{\xi}} = \int_{-\infty}^{+\infty} \frac{d\omega}{2\pi} e^{iz\omega} e^{\sum_{\nu \neq \mu} \frac{q_\nu}{N^\gamma} [\cos(\omega q_\nu m_\nu) - 1]} \quad (44)$$

If $\gamma > 0$, extending the sum in the exponent to all patterns will add a negligible contribution in the thermodynamic limit, hence, as $N \rightarrow \infty$ all clones will have the same noise distribution

$$P_\mu(z|\{m_\nu, q_\nu\}) \rightarrow P_P(z|\mathbf{m}, \mathbf{q}) = \langle \delta(z - \sum_{\nu=1}^P q^\nu \xi^\nu m_\nu) \rangle_{\boldsymbol{\xi}} \quad (45)$$

We note that the sum on the RHS of (45) is at most $\mathcal{O}(\sim N^{\delta-\gamma})$, hence for $\delta < \gamma$ it is negligible in the thermodynamic limit. This yields $P_P(z|\mathbf{m}, \mathbf{q}) \rightarrow \delta(z)$ as $N \rightarrow \infty$, so that equations (43) decouple and the system reduces, for $\delta < \gamma$, to a set of independent Curie-Weiss ferromagnets, each evolving according

$$\frac{dm_\mu}{dt} = \tanh(\beta q_\mu m_\mu) - m_\mu. \quad (46)$$

At the steady state, each B clone μ becomes active at its own critical temperature $T_c = q_\mu$, independently of the other clones (fig. 12, left). In contrast, for $\delta \geq \gamma$ the noise distribution $P_P(z|\mathbf{m}, \mathbf{q})$ has a finite width, due to clonal interference, and the equations for the evolution of clonal activations are coupled. In this regime, clones compete to be activated and the ones with fewer triggered receptors will fail to be switched on (fig. 12, right). In the following section we will analyse the effect of receptors heterogeneity in the regime of competing clones. We will show that clonal interference affects both critical temperature and intensity of B clones activations.

4.2.1. Bifurcations near the critical temperature and stability region in the regime of competing clones. In this section we study the bifurcations away from $\mathbf{m} = (0, \dots, 0)$ below the critical temperature $T_c = q_{\max}$. Without loss of generality, we assume $q_{\max} = q_1$. We Taylor expand the steady state equations obtained by setting $dm_\mu/dt = 0$ in (41), for small m_μ at $\beta q_1 = 1 + \epsilon$

$$m_\mu \simeq \frac{N^\gamma}{q_\mu} \beta \sum_\nu^P q_\nu \langle \xi^\mu \xi^\nu \rangle m_\nu - \frac{N^\gamma}{q_\mu} \frac{\beta^3}{3} \sum_{\nu\rho\lambda}^P q_\nu q_\rho q_\lambda \langle \xi^\mu \xi^\nu \xi^\rho \xi^\lambda \rangle m_\nu m_\rho m_\lambda = \quad (47)$$

$$= \beta q_\mu m_\mu - \frac{\beta^3 q_\mu^3}{3} m_\mu^3 - \beta \frac{q_\mu}{N^\gamma} m_\mu \sum_{\rho \neq \mu}^P m_\rho^2 q_\rho^3. \quad (48)$$

For any μ , $m_\mu = 0$ is always a solution. Non-zero solutions are given, for $\mu = 1$, by

$$\beta q_1 - 1 - \frac{\beta^3 q_1^3}{3} m_1^2 + \frac{\beta q_1^4}{N^\gamma} m_1^2 - \frac{\beta^3}{N^\gamma} q_1 \sum_{\rho > 1}^P m_\rho^2 q_\rho^3 = 0 \quad (49)$$

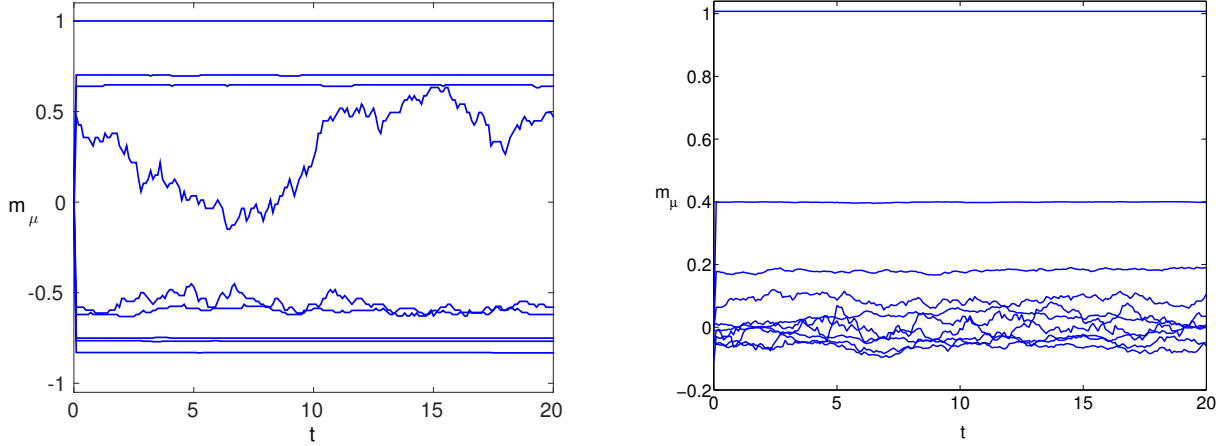


Figure 12. Monte Carlo simulations with $N = 10^4$ spins, $q_\mu = \epsilon^\mu q$. $T = 0.01$, $\epsilon = 0.7$, $q_1 = 6$. Left: $\delta = 0.2, \gamma = 0.25$. In the non-competing regime ($\delta < \gamma$) all clones are activated. Right: $\delta = \gamma = 0.25$. In this case only few clones with the highest number of receptors are active.

that at $\beta q_1 = 1 + \epsilon$ and for large N yield

$$m_1^2 = 3\epsilon - \frac{3}{q_1^2 N^\gamma} \sum_{\rho>1}^P m_\rho^2 q_\rho^3. \quad (50)$$

For $\mu \neq 1$, we have

$$\beta q_\mu - 1 - \frac{\beta^3 q_\mu^3}{3} m_\mu^2 + \frac{\beta q_\mu^4}{N^\gamma} m_\mu^2 - \frac{\beta^3}{N^\gamma} q_\mu \sum_{\rho>1}^P m_\rho^2 q_\rho^3 = 0 \quad (51)$$

which gives, for $N \rightarrow \infty$ and to $\mathcal{O}(\epsilon^0)$,

$$m_\mu^2 = \frac{3}{q_\mu^3} (q_1^2 q_\mu - q_1^3) - \frac{3}{N^\gamma q_\mu^2} \sum_{\rho>1}^P m_\rho^2 q_\rho^3 + \mathcal{O}(N^{-\gamma}). \quad (52)$$

Summing over $\mu > 1$ we get

$$\sum_{\mu>1}^P m_\mu^2 q_\mu^3 \left(1 + \frac{3}{N^\gamma} \sum_{\rho>1}^P q_\rho \right) = 3 \left(\sum_{\mu>1}^P (q_\mu - q_1) \right) \quad (53)$$

Since $q_\mu < q_1, \forall \mu > 1$, this equality can never be satisfied, showing that $m_\mu = 0, \forall \mu > 1$. Substituting this result into (50), we find $m_1^2 = 3\epsilon$, hence the first state to bifurcate away from $\mathbf{m} = (0, \dots, 0)$ is $\mathbf{m} = (\sqrt{3\epsilon}, 0, \dots, 0)$. Next we calculate the region where the pure state $(m_1, 0, \dots, 0)$ stays stable, by inspecting the sign of the eigenvalues of the Jacobian of the linearised equations of motion about the steady state.

For a steady state with the general structure $\mathbf{m} = (m_1, m_2, \dots, m_n, 0, \dots, 0)$, where n is the fraction of activated clones, the Jacobian (23) has a block structure, where diagonal terms are,

for $\mu \leq n$

$$J_{\mu\mu} = \beta q_\mu (1 - \langle \tanh^2(\beta(q_\mu m_\mu + \sum_{\nu \neq \mu}^n \xi^\nu q_\nu m_\nu)) \rangle_{\boldsymbol{\xi}}) - 1 \quad (54)$$

and for $\mu > n$

$$J_{\mu\mu} = \beta q_\mu (1 - \langle \tanh^2(\beta \sum_{\nu}^n \xi^\nu q_\nu m_\nu) \rangle_{\boldsymbol{\xi}}) - 1, \quad (55)$$

while off-diagonal elements are, for $\mu, \nu \leq n$

$$J_{\mu\nu} = -\frac{\beta q_\mu}{N^\gamma} \langle \tanh^2(\beta \sum_{\nu}^n \xi^\nu q_\nu m_\nu) \rangle_{\boldsymbol{\xi}} - 1 \quad (56)$$

and $J_{\mu\nu} = 0$ otherwise. For $N \rightarrow \infty$ the matrix becomes diagonal with eigenvalues $\lambda_\mu = J_{\mu\mu}$ given by (54) for $\mu \leq n$ and (55) for $\mu > n$. In the pure state $\mathbf{m}^* = (m_1, 0, \dots, 0)$, where only one clone is activated, we have

$$\lambda_1 = \beta q_1 (1 - \langle \tanh^2(\beta q_1 m_1) \rangle_{\boldsymbol{\xi}}) - 1, \quad (57)$$

$$\lambda_\mu = \beta q_\mu (1 - \langle \tanh^2(\beta \xi^1 q_1 m_1) \rangle_{\boldsymbol{\xi}}) - 1 \quad \mu > 1. \quad (58)$$

Near the critical temperature $T_c = q_1$, setting $\beta q_1 = 1 + \epsilon$ and using $m_1^2 \simeq 3\epsilon$ gives

$$\lambda_1 = \beta q_1 - 1 - \beta^3 m_1^2 q_1^3 = -2\epsilon < 0 \quad (59)$$

$$\lambda_\mu = \beta q_\mu - 1 - \beta^3 q_1^2 q_\mu \langle \xi_1^2 m_1^2 \rangle_{\boldsymbol{\xi}} = (1 + \epsilon) \frac{q_\mu}{q_1} - 1, \quad \mu > 1 \quad (60)$$

showing that for $q_\mu < q_1$ the pure state is stable near criticality, as opposed to the case $q_\mu = q_1, \forall \mu$ studied in [6], where all clones are activated with the same intensity below T_c . In the opposite limit $T \rightarrow 0$, we get from (57), (58)

$$\lambda_1 \simeq -1, \quad (61)$$

$$\lambda_\mu \simeq \beta q_\mu \left(1 - \frac{q_1}{N^\gamma}\right) - 1 \simeq \beta q_\mu - 1. \quad (62)$$

showing that the pure state is unstable at low temperature.

Indeed, as the temperature is lowered below q_1 , we expect clones with fewer receptors to get active. In particular, at $T = 0$ we expect all clones to be activated, in a hierarchical fashion, whereby the system sends the highest possible signal to the clone with maximum number of receptors, the clone with second highest number of receptors is signalled by the remaining $N - q_1 N^{1-\gamma}$ spare T cells and so on. This leads to the following heuristic rule for noiseless clone activations

$$m_\mu = \prod_{j=1}^{\mu-1} \left(1 - \frac{q_j}{N^\gamma}\right), \quad \mu = 1, \dots, P, \quad (63)$$

in agreement with Monte Carlo simulations shown in fig. 13.

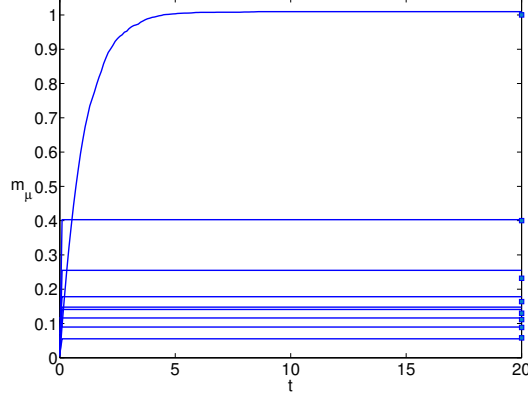


Figure 13. Monte Carlo simulations with $N = 10^4$ spins, $q_\mu = \epsilon^\mu q$. $T = 0.001$, $\epsilon = 0.7$, $q_1 = 6$, $\delta = \gamma = 0.25$. The markers represents the theoretical predictions at $T = 0$ (63).

4.2.2. Sequential B-clones activation: critical temperature and interference effects. In this section we calculate the critical temperature at which clones $\mu > 2$ with fewer receptors get activated. We focus on the regime of clonal interference $\delta \geq \gamma$, as for $\delta < \gamma$ each clone μ gets active at its own critical temperature $T_\mu = q_\mu$. Without loss of generality we can set $P = \alpha N^\gamma$ for $\delta \geq \gamma$, where $\alpha = 1$ for $\delta = \gamma$ and $\alpha \rightarrow \infty$ for $\delta > \gamma$. In the following we will consider $q_1 > q_2 > \dots > q_P$. Assuming that \mathbf{m} bifurcates continuously from the pure state, we can Taylor expand (41) at the steady state for small m_ν , with $\nu \neq 1$, while $m_1 = \mathcal{O}(1)$. For $\mu \neq 1$ we have

$$\begin{aligned} m_\mu &= \frac{N^\gamma}{q_\mu} \left\langle \xi^\mu \tanh \left(\beta (\xi^1 q_1 m_1 + \sum_{\nu=2}^P q_\nu \xi^\nu m_\nu) \right) \right\rangle_{\xi} \\ &= \left\langle \xi^\mu \tanh \left(\beta \sum_{\nu=2}^P q_\nu \xi^\nu m_\nu \right) \right\rangle_{\xi, \xi^\mu \neq 0} + \mathcal{O}(N^{-\gamma}) \end{aligned} \quad (64)$$

$$\begin{aligned} &\simeq \beta \sum_{\nu=2}^P q_\nu \langle \xi^\mu \xi^\nu \rangle_{\xi^\mu \neq 0} m_\nu - \beta^3 \sum_{\rho \neq \nu}^P \langle \xi^\mu \xi^\nu \xi^\rho \xi^\lambda \rangle_{\xi^\mu \neq 0} m_\nu m_\rho m_\lambda q_\nu q_\rho q_\lambda . \\ &\simeq \beta q_\mu m_\mu - \frac{\beta^3 q_\mu^3}{3} m_\mu^3 - \frac{\beta^3 q_\mu m_\mu}{N^\gamma} \sum_{\rho \neq \mu}^P q_\rho^3 m_\rho^2 . \end{aligned} \quad (65)$$

The solutions are $m_\mu = 0$, or

$$1 = \beta q_\mu - \frac{\beta^3 q_\mu^3}{3} m_\mu^2 - \frac{\beta^3 q_\mu}{N^\gamma} \sum_{\rho \neq \mu}^P q_\rho^3 m_\rho^2 . \quad (66)$$

Hence, for $1 - \beta q_\mu > 0$, $m_\mu = 0$ while for $1 - \beta q_\mu < 0$ the μ -th clone may be activated. Hence, the first state to bifurcate away from the pure state is $\mathbf{m} = (m_1, m_2, 0, \dots, 0)$ at $T = q_2$. Its amplitude

at $\beta q_2 = 1 - \epsilon$ is

$$m_2^2 \simeq 3\epsilon - \frac{3q_1^3}{q_2^2 N^\gamma} m_1^2 \quad (67)$$

i.e. $m_2^2 = 3\epsilon + \mathcal{O}(N^{-\gamma})$. As T is lowered below q_2 we expect that the clones will activate sequentially one after the other, each one at its own temperature. In particular, assuming $m_{1,2} = \mathcal{O}(1)$, we have for $\mu > 2$

$$m_\mu = \left\langle \xi^\mu \tanh \left(\beta \sum_{\nu>3}^P q_\nu \xi^\nu m_\nu \right) \right\rangle_{\xi, \xi^\mu \neq 0} + \mathcal{O}(N^{-\gamma}) \quad (68)$$

and expanding for $m_{\nu>2}$ small at $T < q_2$ shows that m_3 becomes non-zero at $T = q_3 + \mathcal{O}(N^{-\gamma})$. Generalizing for $n \ll N^\gamma$ activated clones $m_1, \dots, m_n = \mathcal{O}(1)$ we have for $\mu > n$

$$m_\mu = \left\langle \xi^\mu \tanh \left(\beta \sum_{\nu>n}^P q_\nu \xi^\nu m_\nu \right) \right\rangle_{\xi, \xi^\mu \neq 0} + \mathcal{O}(nN^{-\gamma}) \quad (69)$$

giving as bifurcation temperature $T_n = q_n + \mathcal{O}(nN^{-\gamma})$. As the number of activated clones increases, their cumulative effect on the activation temperature of the remaining clones increases and can no longer be neglected for $n = \mathcal{O}(N^\gamma)$. The activation temperature of pattern $n + 1$, when $n \sim N^\gamma$ clones have been activated, can be worked out from

$$m_{n+1} = \left\langle \tanh \left(\beta (q_{n+1} m_{n+1} + \sum_{\nu=1}^n q_\nu \xi^\nu m_\nu) \right) \right\rangle_{\xi}, \quad (70)$$

that gives, upon insertion of $\int dz \delta(z - \sum_{\nu=1}^n q_\nu \xi^\nu m_\nu) = 1$

$$m_{n+1} = \int dz P_n(z | \mathbf{m}, \mathbf{q}) \tanh(\beta(q_{n+1} m_{n+1} + z)). \quad (71)$$

with $P_n(z | \mathbf{m}, \mathbf{q})$ defined in (45). Taylor expanding for m_{n+1} small we have, to leading orders

$$m_{n+1} = \int dz P_n(z | \mathbf{m}, \mathbf{q}) \left[(1 - \tanh^2(\beta z)) \beta q_{n+1} m_{n+1} + \mathcal{O}(m_{n+1}^2) \right] \quad (72)$$

where we have used $P_n(z | \mathbf{m}, \mathbf{q}) = P_n(-z | \mathbf{m}, \mathbf{q})$. A solution is $m_{n+1} = 0$ and a non-zero solution is possible for

$$\beta q_{n+1} = \frac{1}{1 - \int dz P_n(z | \mathbf{m}, \mathbf{q}) \tanh^2(\beta z)}. \quad (73)$$

For $n \ll N^\gamma$, $P_n(z | \mathbf{m}, \mathbf{q}) = \delta(z)$, and we retrieve $\beta q_{n+1} = 1$ for the temperature at which m_{n+1} becomes non-zero. For $P_n(z | \mathbf{m}, \mathbf{q})$ having a small but finite width we can use $\tanh(\beta z) \simeq \beta z$

$$\beta q_{n+1} \simeq 1 + \frac{\langle z^2 \rangle}{q_{n+1}^2} \simeq 1 + \frac{\sum_{\mu=1}^n q_\mu^3 m_\mu^2}{q_{n+1}^2 N^\gamma}, \quad (74)$$

showing that $T_{n+1} < q_{n+1}$ and deviations from q_{n+1} depend on the promiscuity distribution of the activated clones. Equation (73) shows that as more clones are activated, these create an interference, encoded in $P_n(z | \mathbf{m}, \mathbf{q})$, that decreases the activation temperature of the inactive ones. Furthermore, it suggests that the number n of clones that the system can activate (*i.e.* the number of $\mathcal{O}(1)$ order parameters m_μ) at small but finite temperature is $\mathcal{O}(N^\gamma)$.

4.2.3. *Numerical examples.* In this section we test (73) and look at the effect of receptors' heterogeneity on the intensity of B clones activation, for three simple cases that can be treated analytically, with $q_1 > q_2$ and $P = \alpha N^\gamma$:

- (i) $\mathbf{q} = (q_1, q_2, \dots, q_2)$: only one clone has a higher number of receptor;
- (ii) $\mathbf{q} = (q_1, \dots, q_1, q_2, \dots, q_2)$: half of the clones have promiscuity q_1 , and half have promiscuity q_2 ;
- (iii) $\mathbf{q} = (q_1, \dots, q_1, q_2)$: only one clone has a smaller number of receptors.

Our goal is to analyse the increasing interference effect due to the activated clones with more receptors on the quiescent ones with less receptors. According to (73) active clones should play the role of interference terms that lower the critical temperature of the quiescent clones.

- (i) Clones with the same number of receptors will be activated with the same intensity [6] and the activation vector bifurcating away from the pure state will have the form (see Sec. 5.2.1 for a rigorous derivation) $\mathbf{m} = (m_1, m_2, \dots, m_2)$. The amplitudes m_1 and m_2 are found from

$$\begin{aligned}
m_1 &= \frac{N^\gamma}{q_1} \left\langle \xi^1 \tanh \left(\beta (\xi^1 q_1 m_1 + q_2 \sum_{\nu=2}^P \xi^\nu m_\nu) \right) \right\rangle_{\boldsymbol{\xi}} \\
&= \left\langle \tanh \left(\beta (q_1 m_1 + q_2 m_2 \sum_{\nu=2}^P \xi^\nu) \right) \right\rangle_{\boldsymbol{\xi}} \\
&= \sum_z P_{P-1}(z|\mathbf{q}) \tanh \beta (q_1 m_1 + q_2 m_2 z)
\end{aligned} \tag{75}$$

and

$$\begin{aligned}
m_2 &= \sum_z P_{P-2}(z|\mathbf{q}) \tanh \beta [q_1 \xi^1 m_1 + q_2 m_2 (1+z)] \\
&= \sum_z P_{P-2}(z|\mathbf{q}) \tanh \beta [q_2 m_2 (1+z)] + \mathcal{O}(N^{-\gamma})
\end{aligned} \tag{76}$$

where

$$P_n(z|\mathbf{q}) = \left\langle \delta(z - \sum_1^n \xi^\nu) \right\rangle_{\boldsymbol{\xi}}. \tag{77}$$

Using (44), we can write $P_P(z|\mathbf{q}) = e^{-q_2 \alpha} I_z(q_2 \alpha)$ where $I_z(x)$ is the modified Bessel function of the first kind [26], and $P_{P-1}(z|\mathbf{q}) \simeq P_{P-2}(z|\mathbf{q}) \simeq P_P(z|\mathbf{q})$. The activation temperature of the clones with smaller promiscuity follows from Taylor expansion of (76) for small m_2 giving

$$\begin{aligned}
m_2 &= \sum_z P_{P-2}(z|\mathbf{q}) [\beta q_2 m_2 (1+z) - \frac{1}{3} (\beta q_2 m_2)^3 (1+z)^3] + \mathcal{O}(N^{-\gamma}) \\
&= \beta q_2 m_2 - \frac{1}{3} (\beta q_2 m_2)^3 (1 + 3\langle z^2 \rangle) + \mathcal{O}(N^{-\gamma}) \\
&= \beta q_2 m_2 - \frac{1}{3} (\beta q_2 m_2)^3 (1 + 3\alpha q_2) + \mathcal{O}(N^{-\gamma})
\end{aligned} \tag{78}$$

where we used the parity of $P_n(z|\mathbf{q}) = P_n(-z|\mathbf{q}) \forall n$ and $\langle z^2 \rangle \equiv \sum_z P_P(z|\mathbf{q}) z^2 = \alpha q_2$. We retrieve $\beta q_2 = 1 + \mathcal{O}(N^{-\gamma})$ for the activation temperature of m_2 , consistently with (73), for $n = 1$. The activation intensity at $\beta q_2 = 1 + \epsilon$ follows from (78) as

$$m_2 = \frac{3\epsilon}{1 + 3q_2\alpha}, \quad (79)$$

as one expects for homogeneous clones in the absence of clone $\mu = 1$ [6]. In fig. 14 we plot the amplitudes m_1, m_2 resulting from (75), (76), as a function of the temperature (left) and those resulting from Monte Carlo simulations, as a function of time (right). The latter are seen to relax to the theoretically predicted steady state. A contour plot of $m_2 = 0$ in the

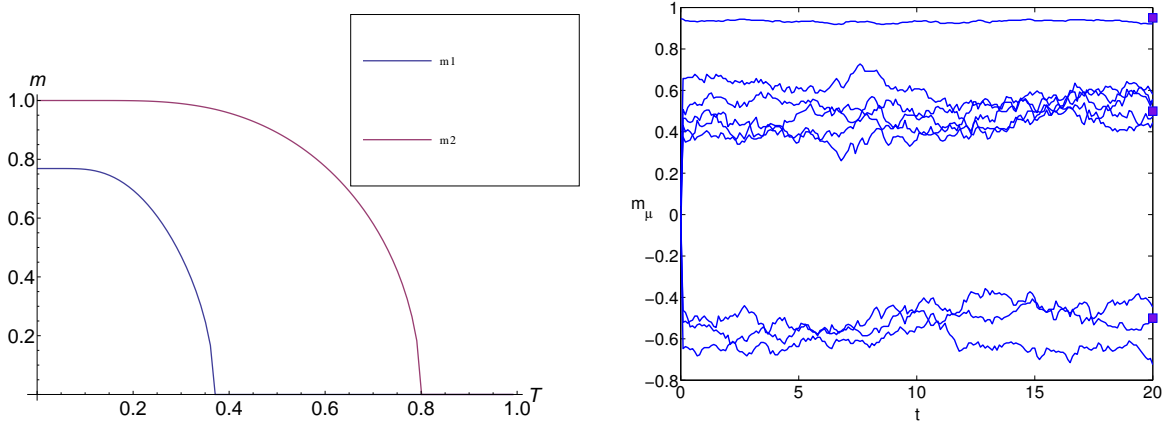


Figure 14. Left: steady state solutions m_1, m_2 of the dynamical system (75), (76), as function of the temperature T , for $q_1 = 0.8, q_2 = 0.4$. Right: Monte Carlo simulations with $N = 10^4$ spins, $\delta = \gamma = 0.25, T = 0.3, q_1 = 0.8, q_2 = 0.4$. The markers are the theoretically predicted steady state activations (75), (76).

$T - q_2$ plane, computed numerically from (76), is shown in fig. 15. Deviations from the line $T = q_2$ are consistent with finite size effects $N^{-\gamma}$.

In conclusion, the presence of one clone with a higher number of receptors, does not affect, in the thermodynamic limit, the activation temperature nor the activation intensity of clones with fewer receptors.

- (ii) In this case we expect a transition from the state $\mathbf{m} = (m_1, \dots, m_1, 0, \dots, 0)$ to $\mathbf{m} = (m_1, \dots, m_1, m_2, \dots, m_2)$, with

$$\begin{aligned} m_1 &= \sum_{z_1, z_2} P_{P/2}(z_1|\mathbf{q}) P_{P/2}(z_2|\mathbf{q}) \tanh(\beta(q_1 m_1(1 + z_1) + q_2 m_2 z_2)) , \\ m_2 &= \sum_{z_1, z_2} P_{P/2}(z_1|\mathbf{q}) P_{P/2}(z_2|\mathbf{q}) \tanh(\beta(q_2 m_2(1 + z_2) + q_1 m_1 z_1)) , \end{aligned} \quad (80)$$

The temperature at which the on-set of non-zero m_2 occurs is found by Taylor expanding

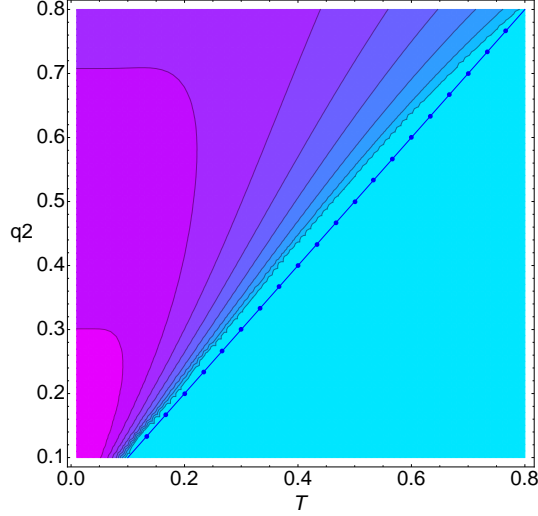


Figure 15. Contours of constant m_2 with $\mathbf{q} = (q_1, q_2, \dots, q_2)$. The contour indicating the on-set of a non-zero value of m_2 is very close to the blue dotted line $T = q_2$ theoretically predicted. Deviations are within finite size effects $\mathcal{O}(N^{-\gamma})$.

(80) for small m_2 with $m_1 = \mathcal{O}(1)$

$$\begin{aligned}
m_2 &= \sum_{z_1, z_2} P_{P/2}(z_1|\mathbf{q})P_{P/2}(z_2|\mathbf{q}) [\tanh(\beta q_1 m_1 z_1) + (1 - \tanh^2(\beta q_1 m_1 z_1))\beta q_2 m_2(1 + z_2) + \mathcal{O}(m_2^2)] \\
&= \beta q_2 m_2 \sum_{z_1} P_{P/2}(z_1|\mathbf{q})(1 - \tanh^2(\beta q_1 m_1 z_1))
\end{aligned} \tag{81}$$

giving $m_2 \neq 0$ for

$$\beta q_2 = \frac{1}{1 - \sum_z P_{P/2}(z|\mathbf{q}) \tanh^2(\beta q_1 m_1 z)}. \tag{82}$$

The theoretically predicted critical line (82) is in excellent agreement with the contour plot of $m_2 \neq 0$ in the $T - q_2$ plane, shown in fig. 16 (left), computed numerically from (80). The plot shows that in the presence of $\mathcal{O}(N^\gamma)$ clones with higher numbers of receptors, the activation temperature of those with smaller promiscuity q_2 will deviate from the line $T = q_2$.

(iii) This is the case where deviations from the line $T = q_2$ are expected to be largest. From (41) we have

$$\begin{aligned}
m_1 &= \frac{N^\gamma}{q_1} \left\langle \xi^1 \tanh \left(\beta (\xi^1 q_1 m_1 + \sum_{\nu=2}^P q_\nu \xi^\nu m_\nu) \right) \right\rangle_{\xi} \\
&= \left\langle \tanh \left(\beta (q_1 m_1 + \sum_{\nu=2}^P q_\nu \xi^\nu m_\nu) \right) \right\rangle_{\xi} \\
&= \sum_z P_{P-2}(z|\mathbf{q}) \tanh[\beta (q_1 m_1 (1 + z) + q_2 m_2 \xi^n)] \\
&= \sum_z P_{P-2}(z|\mathbf{q}) \tanh[\beta q_1 m_1 (1 + z)] + \mathcal{O}(N^{-\gamma})
\end{aligned} \tag{83}$$

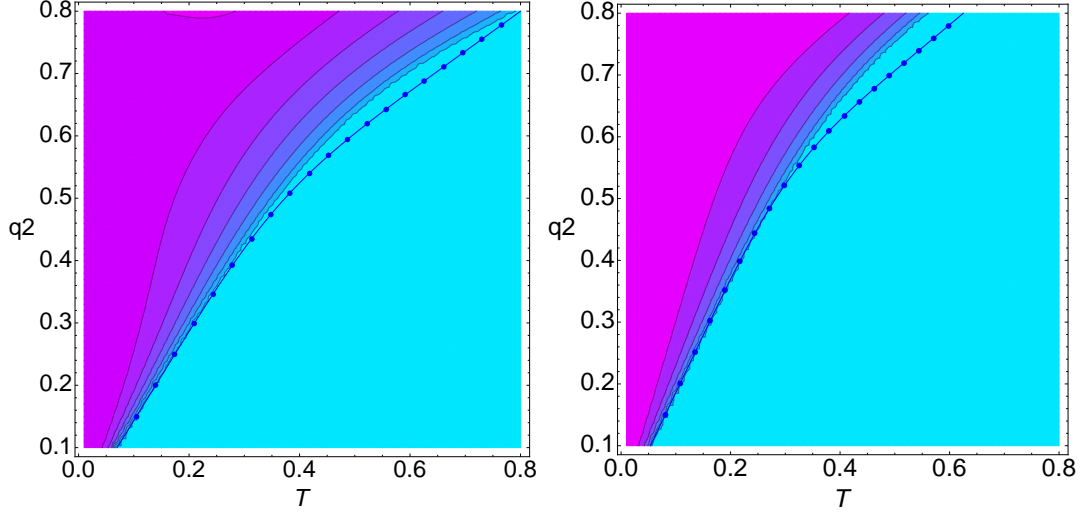


Figure 16. Contour plot of m_2 in the (T, q_2) plane for $\mathbf{q} = (q_1, \dots, q_1, q_2, \dots, q_2)$ (left) and $\mathbf{q} = (q_1, \dots, q_1, q_2)$ (right). The blue dotted line represents the theoretical critical temperature line computed using respectively the self-consistent equations (80) (left) and (83)(right) together with the theoretical predictions for the critical temperature (82)(left) and (86)(right). Deviations from the numerical results when $q_2 \simeq q_1$ are due to the fact that (73) is obtained assuming $m_2 \ll m_1$, condition which is not satisfied when $q_2 \simeq q_1$.

and

$$\begin{aligned}
m_2 &= \left\langle \tanh \left(\beta(q_2 m_2 + \sum_{\nu \neq 2}^P q_\nu \xi^\nu m_\nu) \right) \right\rangle_{\xi} \\
&= \sum_z P_{P-1}(z|\mathbf{q}) \tanh[\beta(q_2 m_2 + q_1 m_1 z)]
\end{aligned} \tag{84}$$

When clones with fewer receptors get active, we expect $m_1 = \mathcal{O}(1)$ and m_2 small. Taylor expanding for m_2 small and using the parity of $P_n(z|\mathbf{q}) = P_n(-z|\mathbf{q}) \forall n$

$$\begin{aligned}
m_2 &= \sum_z P_{P-1}(z|\mathbf{q}) [\tanh(\beta q_1 m_1 z) + (1 - \tanh^2(\beta q_1 m_1 z)) \beta q_2 m_2] + \mathcal{O}(m_2^2) \\
&= \beta q_2 m_2 [1 - \sum_z P_{P-1}(z|\mathbf{q}) \tanh^2(\beta q_1 m_1 z)] + \mathcal{O}(m_2^2)
\end{aligned} \tag{85}$$

we obtain for the activation temperature of the only clone with lowest number of receptors

$$\beta q_2 = \frac{1}{1 - \sum_z P_{P-1}(z|\mathbf{q}) \tanh^2(\beta q_1 m_1 z)} \tag{86}$$

in agreement with the contour plot of $m_2 \neq 0$ in the $T - q_2$ found numerically, shown in fig. 16 (right). Deviations are compatible with finite size effects and are largest for $q_2 \simeq q_1$ where the assumption $m_2 \ll m_1$ is no longer valid. Monte Carlo simulations with 10 B clones, one of which has a lower promiscuity $q_2 = 0.6$, are shown in fig. 17: at $T = q_2$ the pattern with lowest receptors is inactive and it is activated only at a much lower temperature $T \simeq 0.2$.

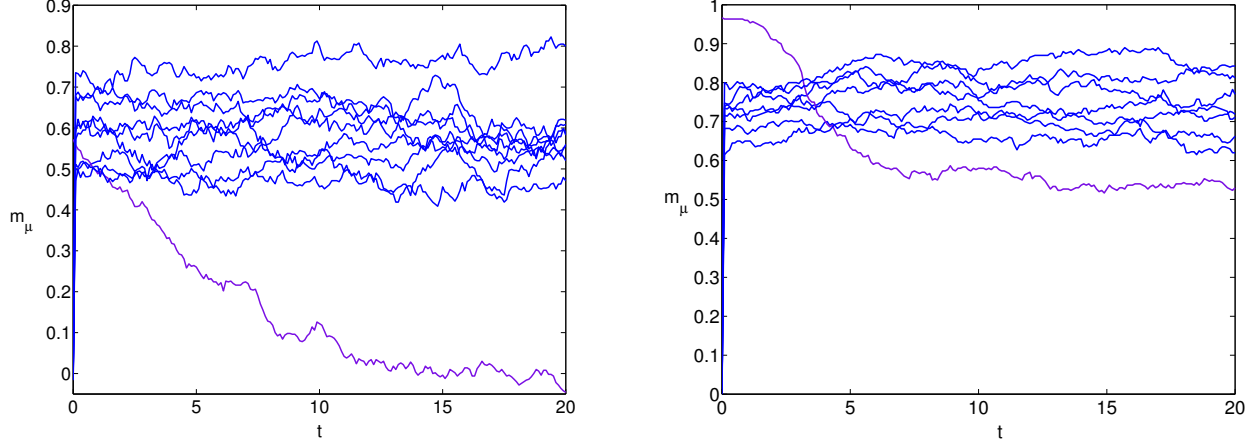


Figure 17. Time evolution of B clones activation in Monte Carlo simulations with 10^4 spins and $\mathbf{q} = (q_1, \dots, q_1, q_2)$ (case (iii)) with $q_1 = 0.8$ (blue) and $q_2 = 0.6$ (violet). The activation for the clone with less receptors (violet) decays to 0 for $T = 0.5$ (left) and stays non-zero for $T = 0.2$ (right), *i.e.* at temperatures considerably lower than that in the absence of clonal interference $T = q_2$.

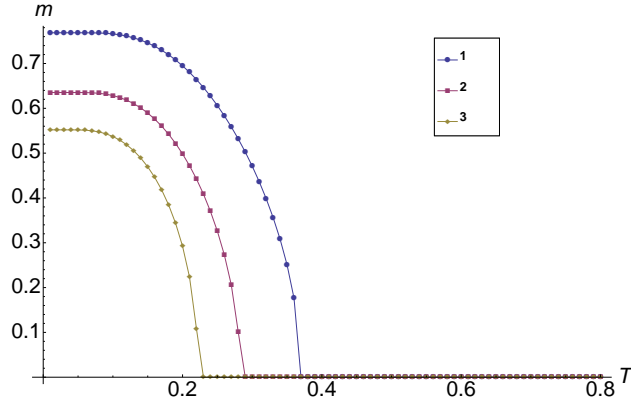


Figure 18. Plot of m_2 as a function of T in the different cases: (1) $\mathbf{q} = (q_1, q_2, \dots, q_2)$, (2) $\mathbf{q} = (q_1, \dots, q_1, q_2, \dots, q_2)$, (3) $\mathbf{q} = (q_1, \dots, q_1, q_2)$. Increasing the interference due to clones activated at a higher temperature, the m_2 intensity decreases.

Finally in fig. 18 we plot m_2 as a function of the temperature in the three different cases with promiscuity (i) $\mathbf{q} = (q_1, q_2, \dots, q_2)$, (ii) $\mathbf{q} = (q_1, \dots, q_1, q_2, \dots, q_2)$, (iii) $\mathbf{q} = (q_1, \dots, q_1, q_2)$. The presence of clones with higher promiscuity q_1 and activation intensity m_1 , does not only affect the activation temperature of clones with lower promiscuity $q = q_2$, but also the intensity m_2 of their immune responses. In conclusion, clones with fewer triggered receptors are activated at a lower temperature and will produce a weaker response than clones with a higher number of active receptors.

5. Idiotypic interactions

In this section we study the effect of the idiotypic interactions on the ability of the system to activate multiple clones in parallel. For simplicity, here we will assume homogeneous receptor promiscuities *i.e.* $q_\mu = c$, $\forall \mu$, so that the dynamical equations (18) read

$$\frac{dm_\mu}{dt} = \frac{N^\gamma}{c} \langle \xi^\mu \tanh(\beta c \sum_{\rho\nu} \xi^\nu (\mathbf{A}^{-1})_{\rho\nu} m_\rho) \rangle \xi - m_\mu \quad (87)$$

Matrix A is positive definite for $k \in (0, 1)$ and symmetric, hence the free-energy of the system is a Lyapunov function for the dynamics [27] and the system will converge to a steady state. Next, we compute the critical temperature at which clonal activation emerges in the steady state

$$m_\mu = \frac{N^\gamma}{c} \langle \xi^\mu \tanh(\beta c \sum_{\rho\nu} \xi^\nu (\mathbf{A}^{-1})_{\rho\nu} m_\rho) \rangle \xi. \quad (88)$$

By summing over $\sum_{\mu\lambda} m_\lambda (\mathbf{A}^{-1})_{\lambda\mu}$

$$\sum_{\mu\lambda} m_\lambda (\mathbf{A}^{-1})_{\lambda\mu} m_\mu = \frac{N^\gamma}{c} \langle \sum_{\mu\lambda} m_\lambda (\mathbf{A}^{-1})_{\lambda\mu} \xi^\mu \tanh(\beta c \sum_{\rho\nu} \xi^\nu (\mathbf{A}^{-1})_{\rho\nu} m_\rho) \rangle \xi \quad (89)$$

using the inequality $|\tanh(x)| \leq |x|$ and averaging over the disorder we obtain

$$\sum_{\mu\lambda} m_\lambda (\mathbf{A}^{-1})_{\lambda\mu} m_\mu \leq \beta c \sum_{\rho\lambda} m_\lambda (\mathbf{A}^{-2})_{\lambda\rho} m_\rho \quad (90)$$

Next we diagonalise the matrix \mathbf{A} by means of the similarity transformation $\mathbf{D} = \mathbf{P}^{-1} \mathbf{A} \mathbf{P}$, where \mathbf{D} is the diagonal matrix constructed from the eigenvalues $\{\mu_\rho\}_{\rho=1}^P$ of \mathbf{A} and \mathbf{P} is the matrix of eigenvectors, which is unitary, *i.e.* $\mathbf{P}^{-1} = \mathbf{P}^T$, since \mathbf{A} is symmetric. Hence, we can rewrite the equation above for the transformed vector $\mathbf{v} = \mathbf{P}^{-1} \mathbf{m}$ as

$$\mathbf{v}^T \mathbf{D}^{-1} \mathbf{v} - \beta c \mathbf{v}^T \mathbf{D}^{-2} \mathbf{v} \leq 0 \quad (91)$$

which gives

$$\sum_{\nu} \left(\frac{v_\nu}{\mu_\nu} \right)^2 (\beta c - \mu_\nu) \geq 0 \quad (92)$$

yielding $\mathbf{v} = \mathbf{0}$ for $\beta c < \mu_{\min}$, where $\mu_{\min} = \min_{\nu} \mu_\nu$. The eigenvalues of \mathbf{A} are

$$\mu_1 = 1 - k, \quad \text{deg}(\mu_1) = P/2 \quad (93)$$

$$\mu_2 = 1 + k, \quad \text{deg}(\mu_2) = P/2 \quad (94)$$

hence, above the critical temperature $T_c = c(\mu_{\min})^{-1} = c/(1 - k)$ we have $\mathbf{m} = \mathbf{0}$, whereas below criticality $\mathbf{m} \neq \mathbf{0}$ is possible (and expected). Remarkably, the critical temperature increases with k , meaning that idiotypic interactions enhance immune system's activation. Next, we investigate the structure of the states bifurcating away from $\mathbf{m} = \mathbf{0}$ below T_c and their stability.

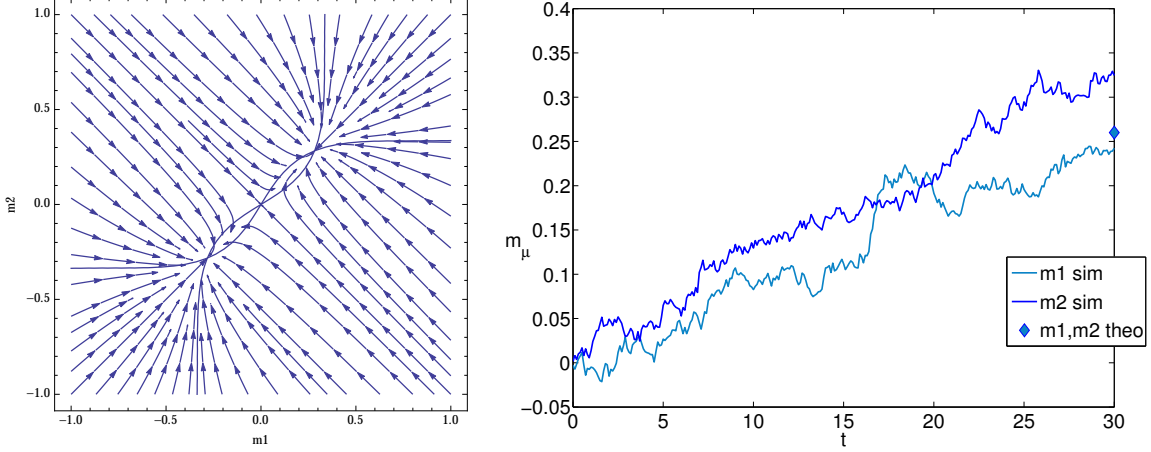


Figure 19. Flow diagram in the plane (m_1, m_2) (left) and Monte Carlo simulations with 10^4 spins (right) for the dynamical system (95) with $T = 1.7$, $c = 0.55$, $k = 0.7$ ($T_c = 1.83$).

5.1. Dynamical equations for two B clones

As before, it is useful to consider first the toy model with $P = 2$ clones. For $k \neq 0$, the dynamics of different clones is always coupled, for all $\gamma \geq 0$. We first look at the case $\gamma = 0$, where the system evolves according to the equations

$$\begin{aligned}
 \frac{dm_1}{dt} &= (1 - c) \tanh \left(\frac{\beta c}{1 - k^2} (m_1 + km_2) \right) + \frac{c}{2} \left[\tanh \left(\frac{\beta c}{1 - k} (m_1 + m_2) \right) \right. \\
 &\quad \left. + \tanh \left(\frac{\beta c}{1 - k} (m_1 - m_2) \right) \right] - m_1 \\
 \frac{dm_2}{dt} &= (1 - c) \tanh \left(\frac{\beta c}{1 - k^2} (km_1 + m_2) \right) + \frac{c}{2} \left[\tanh \left(\frac{\beta c}{1 - k} (m_1 + m_2) \right) \right. \\
 &\quad \left. - \tanh \left(\frac{\beta c}{1 - k} (m_1 - m_2) \right) \right] - m_2
 \end{aligned} \tag{95}$$

The state $\mathbf{m} = (0, 0)$ is a fixed point of the dynamics at all temperatures, but we expect it to become unstable below $T_c = c/(1 - k)$. In order to inspect the structure of the bifurcating state it is convenient to analyse the steady state equations in terms of the variables $x = m_1 + m_2$ and $y = m_1 - m_2$

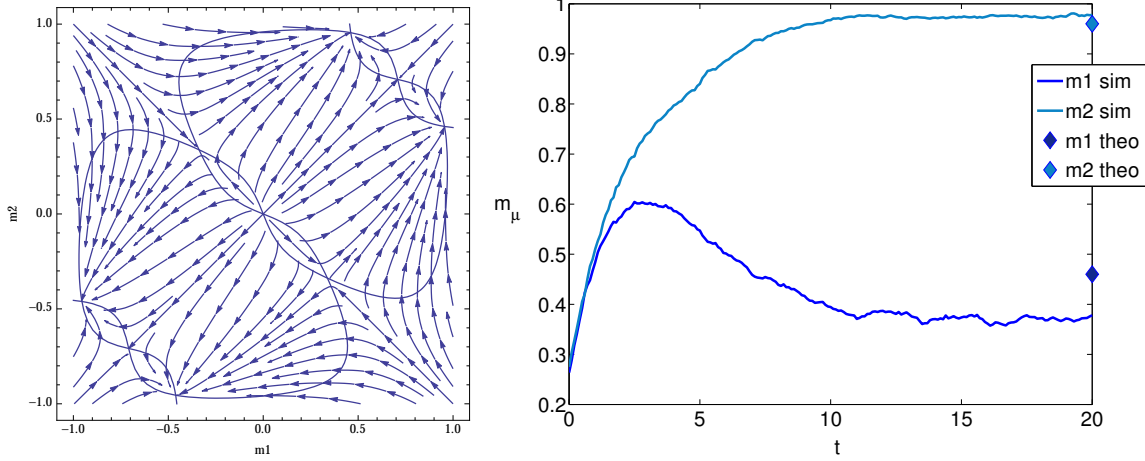


Figure 20. Flow diagram in the plane (m_1, m_2) (left) and Monte Carlo simulations with 10^4 spins (right) for the dynamical system (95), for $T = 0.65, c = 0.55, k = 0.7$ ($T_c = 1.83$).

$$\begin{aligned}
 x &= c \tanh\left(\frac{\beta c x}{1-k}\right) + (1-c) \left[\tanh\left(\frac{\beta c}{1-k^2}(x + (k-1)m_2)\right) \right. \\
 &\quad \left. + \tanh\left(\frac{\beta c}{1-k^2}(x + (k-1)m_1)\right) \right] \\
 y &= c \tanh\left(\frac{\beta c y}{1-k}\right) + (1-c) \left[\tanh\left(\frac{\beta c}{1-k^2}(x + (k-1)m_2)\right) \right. \\
 &\quad \left. - \tanh\left(\frac{\beta c}{1-k^2}(x + (k-1)m_1)\right) \right].
 \end{aligned}$$

Assuming continuous bifurcations, we Taylor expand for small \mathbf{m} near $\beta c = 1 - k$ *i.e.* at $\hat{\beta} \equiv \frac{\beta c}{1-k} = 1 + \epsilon$, obtaining, to leading orders

$$\begin{aligned}
 x &= c\hat{\beta}x - \frac{1}{3}c\hat{\beta}^3x^3 + (1-c)\hat{\beta}x - \frac{1-c}{3(1+k)^2}\hat{\beta}^3x \left[(x + (k-1)m_2)^2 \right. \\
 &\quad \left. + (x + (k-1)m_1)^2 - (x + (k-1)m_1)(x + (k-1)m_2) \right] \quad (96)
 \end{aligned}$$

$$\begin{aligned}
 y &= c\hat{\beta}y - \frac{1}{3}c\hat{\beta}^3y^3 + \frac{(1-c)(1-k)}{(1+k)}\hat{\beta}y - \frac{(1-c)(1-k)}{3(1+k)^3}\hat{\beta}^3y \left[(x + (k-1)m_2)^2 \right. \\
 &\quad \left. + (x + (k-1)m_1)^2 - (x + (k-1)m_1)(x + (k-1)m_2) \right]. \quad (97)
 \end{aligned}$$

We note that $x = y = 0$ is always a solution (corresponding to $\mathbf{m} = (0, 0)$). A solution $y \neq 0$ is not possible as in (97) terms $\mathcal{O}(\epsilon^0)$ do not simplify. Hence, $y = 0$ is the only solution, implying $m_1 = m_2$. In contrast, in (96) first order terms simplify, hence we can have $x \neq 0$. Therefore, mixtures bifurcate from $\mathbf{m} = (0, 0)$ in a symmetric fashion $\mathbf{m} = m(1, 1)$. We can compute the

amplitude m , Taylor expanding (95) at the steady state near T_c , for small m ,

$$m = \hat{\beta}m - \frac{1}{3}\hat{\beta}^3 m^3 - c\hat{\beta}^3 m^3 \quad (98)$$

yielding, at $\hat{\beta} = 1 + \epsilon$,

$$m^2 = \frac{3\epsilon}{1 + 3c} \quad (99)$$

or the trivial solution $m = 0$. Flow diagrams and Monte Carlo simulations are in agreement with theoretical predictions, showing that close to criticality both B clones are activated with the same intensity (fig. 19). Next we investigate the stability of symmetric solutions by computing the eigenvalues of the Jacobian

$$J_{\mu\nu} = \left. \frac{\partial F_{\mu}^{(1)}(\mathbf{m})}{\partial m_{\nu}} \right|_{\mathbf{m}=\mathbf{m}^*}, \quad F_{\mu}^{(1)}(\mathbf{m}) = \frac{N^{\gamma}}{c} \langle \xi^{\mu} \tanh(\beta c \sum_{\rho\lambda} \xi^{\lambda} (\mathbf{A}^{-1})_{\rho\lambda} m_{\rho}) \rangle_{\boldsymbol{\xi}} - m_{\mu}, \quad (100)$$

One has

$$J_{\mu\nu} = \beta c (\mathbf{A}^{-1})_{\mu\nu} (1 - \langle \tanh^2(\beta c \sum_{\rho\lambda} \xi^{\lambda} (\mathbf{A}^{-1})_{\rho\lambda} m_{\rho}^*) \rangle_{\boldsymbol{\xi}}) - \delta_{\mu\nu} + \mathcal{O}(N^{-\gamma}) \quad (101)$$

and substituting $\mathbf{m}^* = m(1, 1)$ we find for the eigenvalues

$$\lambda_1 = \frac{\beta c}{1 - k} - 1 - \frac{\beta c(1 - c)}{1 - k} \tanh\left(\frac{m\beta c}{1 - k}\right)^2 - \beta \frac{c^2}{1 - k} \tanh\left(\frac{2m\beta c}{1 - k}\right)^2, \quad (102)$$

$$\lambda_2 = \frac{\beta c(1 - c)}{1 + k} \left(1 - \tanh\left(\frac{m\beta c}{1 - k}\right)^2\right) + \frac{\beta c^2}{1 - k} - 1. \quad (103)$$

These can be calculated analytically near criticality *i.e.* at $\beta c/1 - k = 1 + \epsilon$ where

$$\lambda_1 = \frac{-2\epsilon - 6\epsilon c}{1 + 3c}, \quad (104)$$

$$\lambda_2 = \frac{-2\epsilon + 6\epsilon c - 2k + 2k\epsilon - 4kc - 4kc\epsilon}{(1 + 3c)(1 + k)}, \quad (105)$$

and for $T \rightarrow 0$, where

$$\lambda_1 = -1, \quad (106)$$

$$\lambda_2 = \frac{\beta c^2}{1 - k} - 1. \quad (107)$$

We deduce that λ_1 is always negative, hence the stability of symmetric solutions is determined by λ_2 . A plot of λ_2 as a function of T is shown in fig. 21 (left) for fixed dilution and B-B interaction strength k . The critical line where $\lambda_2 = 0$ in the $T - c$ plane for different values of k is shown in fig. 21 (right). Remarkably, the region **(S)** where activation of parallel immune responses is accomplished with the same intensity gets wider as k increases. For $\gamma > 0$, the system evolves

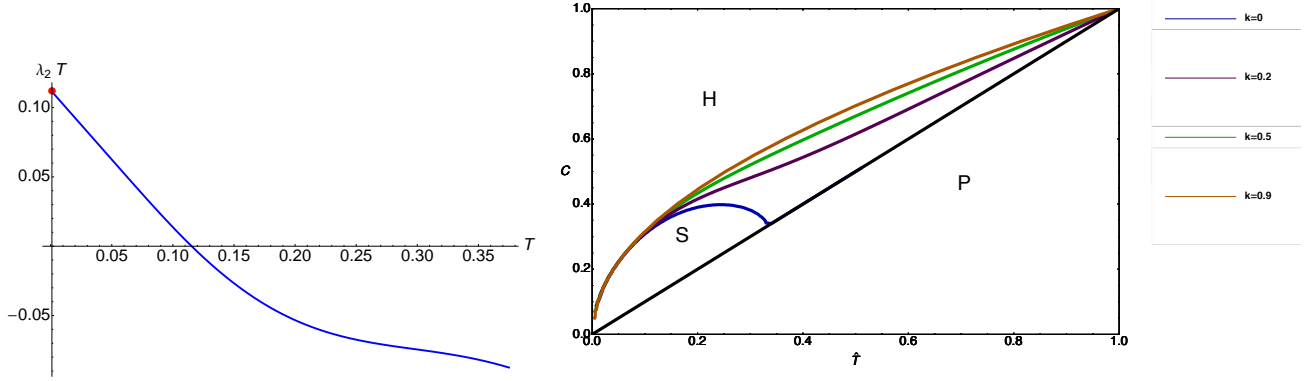


Figure 21. Left: $\lambda_2 T$ as a function of T for $c = 0.3$ and $k=0.2$. The value at $T = 0$ matches the analytical prediction $\lambda_2 T = c^2/1 - k$ (red marker). Right: Contour plot of $\lambda_2 = 0$ with different interaction strengths $k = 0.8, k = 0.5, k = 0.2$ in the parameter space (T, c) . The region where clones are activated in parallel with the same intensity (**S**) becomes wider as k increases.

according to the equations

$$\begin{aligned} \frac{dm_1}{dt} &= \tanh\left(\frac{\beta c}{1 - k^2}(m_1 + km_2)\right) - m_1 \\ \frac{dm_2}{dt} &= \tanh\left(\frac{\beta c}{1 - k^2}(km_1 + m_2)\right) - m_2 \end{aligned} \quad (108)$$

One can show again that $\mathbf{m} = (0, 0)$ is the only fixed point above $T_c = c/(1 - k)$, and symmetric mixtures $\mathbf{m} = m(1, 1)$ bifurcate away from $\mathbf{m} = (0, 0)$ at T_c . Now, however, symmetric mixtures remain stable for any $T < T_c$ (see Sec. 5.2.1), with the intensity m of the symmetric activation found from

$$m = \tanh\left(\frac{\beta cm}{1 - k}\right) \quad (109)$$

Hence for $\gamma > 0$ the system reduces to independent Curie-Weiss ferromagnets, even in the presence of idiotypic interactions, with the critical temperature $T_c = c/(1 - k)$ increasing with the strength of interactions.

5.2. Generalisation to P clones

In this section we turn to the case of $P = N^\delta$, $0 < \delta < 1$ B clones. Again, we expect clones to be activated at $T_c = c/(1 - k)$ in a symmetric fashion. For $\delta < \gamma$ we expect symmetric solutions to be stable for all $T < T_c$, whereas for $\delta \geq \gamma$ we expect them to destabilise at low temperature. Without loss of generality, we can set $P = \alpha N^\gamma$ with $\alpha = 1$ for $\delta = \gamma$ and the cases $\delta < \gamma$ and $\delta > \gamma$ retrieved in the limits $\alpha \rightarrow 0$ and $\alpha \rightarrow \infty$ respectively.

To inspect the behavior of the system near criticality, it is convenient to write the steady

state equations in terms of the rescaled matrix $\hat{A} = A/(1-k)$, with eigenvalues

$$\mu_1 = 1, \quad \text{deg}(\mu_1) = P/2 \quad (110)$$

$$\mu_2 = \frac{1+k}{1-k}, \quad \text{deg}(\mu_2) = P/2. \quad (111)$$

Taylor expanding the steady state equations (88) for small m near T_c , we have, with $\hat{\beta} = \frac{\beta c}{1-k}$,

$$m_\mu \simeq \frac{N^\gamma}{c} \hat{\beta} \sum_{\rho\nu} (\hat{A})_{\rho\nu}^{-1} m_\rho \langle \xi^\mu \xi^\nu \rangle - \frac{\hat{\beta}^3}{3} \frac{N^\gamma}{c} \left[\sum_{\rho_1, \nu_1, \rho_2, \nu_2, \rho_3, \nu_3} \langle \xi^\mu \xi^{\nu_1} \xi^{\nu_2} \xi^{\nu_3} \rangle m_{\rho_1} \hat{A}_{\rho_1 \nu_1} m_{\rho_2} \hat{A}_{\rho_2 \nu_2} m_{\rho_3} \hat{A}_{\rho_3 \nu_3} \right] \quad (112)$$

and averaging over the disorder gives

$$m_\mu = \hat{\beta} \sum_{\rho} (\hat{A})_{\rho\mu}^{-1} m_\rho - \frac{\hat{\beta}^3}{3} \sum_{\rho} (\hat{A})_{\rho\mu}^{-3} m_\rho^3 - \hat{\beta}^3 \frac{c}{N^\gamma} \sum_{\rho} (\hat{A})_{\rho\mu}^{-1} m_\rho \sum_{\tau\pi} (\hat{A})_{\tau\pi}^{-1} m_\pi^2. \quad (113)$$

To make progress, we project m_μ on the eigenvectors of $\hat{\mathbf{A}}^{-1}$: $\hat{\mathbf{A}}^{-1} \mathbf{v}^{(j)} = \mu_j \mathbf{v}^{(j)}$

$$\begin{aligned} \sum_{j=1}^P a_j v_\mu^{(j)} &= \hat{\beta} \sum_{j=1}^P a_j \mu_j v_\mu^{(j)} - \frac{\hat{\beta}^3}{3} \sum_{i,j,k} a_i a_j a_k \mu_i \mu_j \mu_k v_\mu^{(i)} v_\mu^{(j)} v_\mu^{(k)} \\ &- \hat{\beta}^3 \frac{c}{N^\gamma} \sum_i a_i \mu_i v_\mu^{(i)} \sum_{\mu \neq \rho} \sum_{j,k} a_j a_k \mu_j \mu_k v_\rho^{(j)} v_\rho^{(k)} \end{aligned} \quad (114)$$

Next we split the sum into $j = 1, \dots, P/2$ and $j = P/2 + 1, \dots, P$, substitute the eigenvalues (110), (111), and equating linear terms we get

$$\sum_{j=1}^{P/2} a_j v_\mu^{(j)} (1 - \hat{\beta}) + \sum_{j=P/2+1}^P a_j v_\mu^{(j)} \left(1 - \hat{\beta} \frac{1-k}{1+k} \right) = 0 \quad (115)$$

At $\hat{\beta} = 1$ linear terms cancel only if $\sum_{j=P/2+1}^P a_j v_\mu^{(j)} = 0 \forall \mu$, which implies $v_\mu^{(j)} = 0 \forall j = \frac{P}{2} + 1, \dots, P, \forall \mu$. We note that the eigenvectors of \mathbf{A}^{-1} are in the form

$$v_\mu^{(j)} = \frac{1}{2} (m_\mu + m_{\mu+P/2}), \quad j = 1, \dots, P/2, \quad (116)$$

$$v_\mu^{(j)} = \frac{1}{2} (m_\mu - m_{\mu+P/2}), \quad j = P/2 + 1, \dots, P, \quad (117)$$

Therefore we have, for all μ , $m_\mu = m_{\mu+P/2}$ and $v_\mu^{(j)} = m_\mu \forall j = 1, \dots, P/2$. This implies $m_\mu = \sum_{j=1}^P a_j v_\mu^{(j)} = \sum_{j=1}^{P/2} a_j m_\mu$, hence $\sum_{j=1}^{P/2} a_j = 1$. If we plug these conditions into (114)

$$m_\mu (-1 + \hat{\beta}) - \frac{\hat{\beta}^3}{3} m_\mu^3 - \hat{\beta}^3 \frac{c}{N^\gamma} m_\mu \sum_{\rho \neq \mu} m_\rho^2 = 0, \quad (118)$$

we have at $\hat{\beta} = 1 + \epsilon$,

$$m_\mu \epsilon - \frac{1}{3} m_\mu^3 - \frac{c}{N^\gamma} m_\mu |\mathbf{m}|^2 = 0, \quad (119)$$

where $|\mathbf{m}|^2 = \sum_{\rho} m_{\rho}^2$, yielding $m_{\mu} = 0$ or

$$m_{\mu}^2 = 3\epsilon - \frac{3c}{N^{\gamma}} |\mathbf{m}|^2. \quad (120)$$

Each clone activation m_{μ} depends on the whole vector \mathbf{m} , hence all clones will have the same activation strength $m_{\mu} \in (-m, +m, 0)$. Assuming the non-zero components are a fraction $\phi \leq \alpha$ of the total number of components P , we have $|\mathbf{m}|^2 = \alpha\phi N^{\gamma} m^2$ yielding

$$m^2 = \frac{3\epsilon}{1 + 3c\alpha\phi} \quad (121)$$

We will see in the next section that while for $k = 0$ stability of symmetric mixtures is only ensured for $\phi = 1$, in the presence of idiotypic interactions, *i.e.* for $k \neq 0$, values $\phi \neq 1$ are possible.

5.2.1. Linear stability analysis and phase diagram In this section we study the stability of symmetric clonal activation, $\mathbf{m} = m(1, \dots, 1, 0, \dots, 0)$ with $n = \alpha\phi N^{\gamma}$ activated clones, below criticality, in the presence of idiotypic interactions. To this purpose, we study the eigenvalues of the Jacobian of the dynamical system (87), which has a block structure with diagonal elements given for $\mu < n$ by

$$J_{\mu\mu} = \beta(\mathbf{A}^{-1})_{\mu\mu} (1 - \langle \tanh^2[\beta(\sum_{\rho} (\mathbf{A}^{-1})_{\rho\mu} m_{\rho} + \sum_{\rho, \lambda \neq \mu} \xi^{\lambda} (\mathbf{A}^{-1})_{\rho\lambda} m_{\rho})] \rangle_{\xi}) - 1, \quad (122)$$

and for $\mu > n$ by

$$J_{\mu\mu} = \beta(\mathbf{A}^{-1})_{\mu\mu} [1 - \langle \tanh^2 \beta(\sum_{\rho, \lambda \neq \mu} \xi^{\lambda} (\mathbf{A}^{-1})_{\rho\lambda} m_{\rho}) \rangle]_{\xi} - 1, \quad (123)$$

while off-diagonal elements are, for $\mu, \nu \leq n$

$$J_{\mu\nu} = -\frac{\beta(\mathbf{A}^{-1})_{\mu\nu}}{N^{\gamma}} \langle \tanh^2[\beta(\sum_{\rho, \lambda \neq \mu} \xi^{\lambda} (\mathbf{A}^{-1})_{\rho\lambda} m_{\rho})] \rangle_{\xi} - 1] \quad (124)$$

and null otherwise. For $N \rightarrow \infty$ the matrix becomes diagonal and eigenvalues are given by the diagonal elements. At the symmetric fixed point, using $\sum_{\rho} (\mathbf{A}^{-1})_{\rho\lambda} = 1/(1-k) \forall \lambda$, we get

$$\lambda_1 = \frac{\hat{\beta}}{1+k} \left(1 - \sum_z P_n(z) \tanh^2(\hat{\beta}(m(1+z))) \right) - 1 \quad \text{deg}(\lambda_1) = n, \quad (125)$$

$$\lambda_2 = \frac{\hat{\beta}}{1+k} \left(1 - \sum_z P_n(z) \tanh^2(\hat{\beta}mz) \right) - 1 \quad \text{deg}(\lambda_1) = P - n \quad (126)$$

with $P_n(z)$ defined by (77) with $\mathbf{q} = c(1, \dots, 1)$ and given by $P_n(z) = e^{-\alpha\phi c} I_z(\alpha\phi c)$, where $I_z(x)$ is the modified Bessel function of the first kind. Close to criticality, by Taylor expanding in power of $\epsilon = \hat{\beta} - 1$ we obtain

$$\lambda_1 = \frac{-2\epsilon - k(1 + 3c\alpha\phi)}{(1+k)(1 + 3c\alpha\phi)} \quad (127)$$

$$\lambda_2 = \frac{\epsilon - k(1 + 3c\alpha\phi)}{(1+k)(1 + 3c\alpha\phi)}. \quad (128)$$

In contrast to the case $k = 0$ where $\lambda_2 > 0$ and symmetric activation is stable only if it involves *all* clones, in the presence of idiotypic interactions, *i.e.* for $k \neq 0$, both eigenvalues are negative at criticality, showing the emergence of local minima where not all the clones are activated. In the opposite limit, *i.e.* $T \rightarrow 0$ we get

$$\lambda_1 = \frac{\hat{\beta}}{1+k} e^{-\alpha\phi c} I_1(\alpha\phi c) - 1 \quad (129)$$

$$\lambda_2 = \frac{\hat{\beta}}{1+k} e^{-\alpha\phi c} I_0(\alpha\phi c) - 1 \quad (130)$$

For $\delta < \gamma$, $\alpha = 0$, hence using the properties of Bessel functions $I_1(0) = 0$ and $I_0(0) = 1$, we get $\lambda_1 < 0$ and $\lambda_2 > 0$. Since λ_2 has degeneracy $P - n$, symmetric mixtures $\mathbf{m} = m(1, \dots, 1)$ *i.e.* with $n = P$ will be stable for all $T < T_c$. In contrast, for $\delta = \gamma$ *i.e.* $\alpha \neq 0$, $\lambda_1 > 0$ as $I_1(x) > 0$ for any $x > 0$, meaning that symmetric mixtures are unstable at low temperature for any n . Finally, for $\delta > \gamma$ one has $\alpha \rightarrow \infty$, in the thermodynamic limit so $I_n(\alpha\phi c) \simeq (\alpha\phi c)^{-1/2} \forall n$, and symmetric mixtures will gain stability at low temperature as $N \rightarrow \infty$.

Let us now compute the critical line in the phase diagram where symmetric mixtures become unstable. We note that $\lambda_2 > \lambda_1$ for $T \rightarrow 0$ and for $T \rightarrow T_c$, and deduce that $\lambda_2 > \lambda_1$ for all $T < T_c$. Hence, stability of n -mixtures $\mathbf{m} = m(1, \dots, 1, 0, \dots, 0)$ is given by the region where $\lambda_2 < 0$. In fig. 22 (left) we show the critical lines where λ_2 gets zero in the space of scaled parameters $\hat{T} = T/c$, $\hat{\phi} = \phi c$ for different values of k and $\alpha = 1$. As k increases the region where clones are activated with the same intensity gets wider. When λ_2 destabilises, symmetric mixtures can only be stable for $n = P$, *i.e.* for $\phi = 1$, in the region where $\lambda_1 < 0$. A contour plot of $\lambda_1 = 0$ for $\phi = 1$ in the $T - k$ plane is shown in fig. 22 (right).

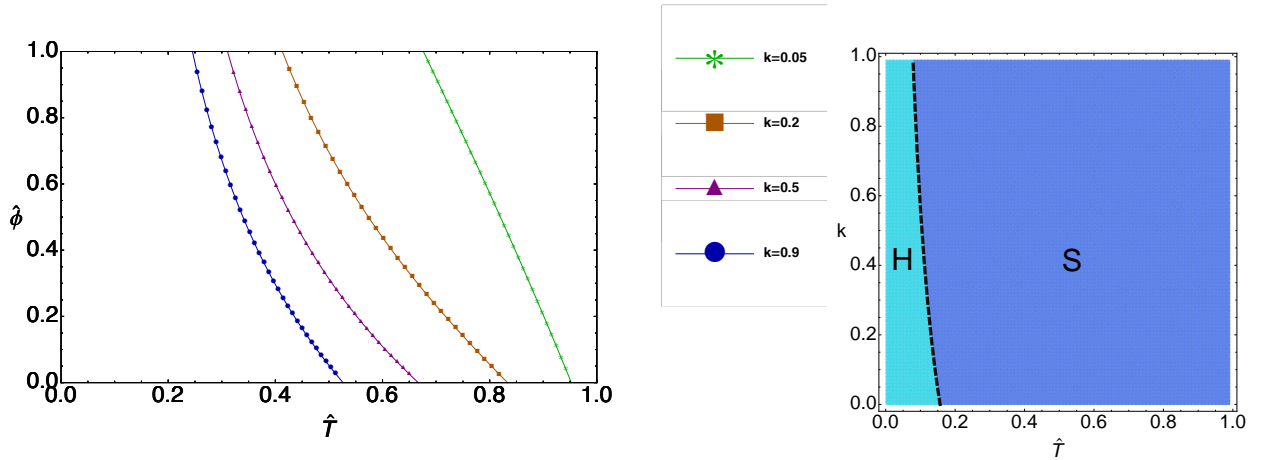


Figure 22. Left: Contour plot of $\lambda_2 = 0$ (obtained from (126)) for $\alpha = 1$, as a function of the scaled parameters ($\hat{T} = T/c$, $\hat{\phi} = \phi c$, for different value of B-B interaction strength k . Increasing k the region where symmetric mixtures are stable (to the right of the critical line) becomes wider. Right: Contour plot of $\lambda_1 = 0$ (obtained from (125)) for $\alpha = \phi = 1$, as a function of the scaled temperature $\hat{T} = T/c$ and strength k of the idiotypic interactions.

6. Antigen effect

In this section we investigate the effect of antigens on the basal activity of the immune system analysed in the previous sections. We will carry out the analysis for homogeneous promiscuities and in the absence of idiotypic interactions. We suppose to have $A = N^a$ antigens, in the presence of which dynamical equations (17) become

$$\frac{dm_\mu}{dt} = \frac{N^\gamma}{c} \langle \xi^\mu \tanh[\hat{\beta} \sum_{\nu=1}^P \xi^\nu (m_\nu + \psi_\nu)] \rangle_{\boldsymbol{\xi}} - m_\mu, \quad (131)$$

where $\hat{\beta} = \beta c$ and ψ_ν is the antigenic field associated to B clone ν . At the steady state we have two sets of equations, those for clones $\mu = 1, \dots, A$ complementary to the incoming viruses and those for non-activated clones $\nu = A + 1, \dots, P$, performing basal activities:

$$m_\mu = \langle \tanh(\hat{\beta}(m_\mu + \psi_\mu + \sum_{\rho \neq \mu}^A \psi_\rho \xi^\rho + \sum_{\rho \neq \mu}^P m_\rho \xi^\rho)) \rangle_{\boldsymbol{\xi}}, \quad \mu = 1, \dots, A, \quad (132)$$

$$m_\nu = \langle \tanh(\hat{\beta}(m_\nu + \sum_{\rho \neq \mu}^A \psi_\rho \xi^\rho + \sum_{\rho \neq \mu}^P m_\rho \xi^\rho)) \rangle_{\boldsymbol{\xi}}, \quad \nu = A + 1, \dots, P. \quad (133)$$

We first look at the case $A \ll N^\gamma$, where the equations can be written as

$$m_\mu = \int dz P(z|\mathbf{m}) \tanh(\hat{\beta}(m_\mu + \psi_\mu + z)), \quad \mu = 1, \dots, A, \quad (134)$$

$$m_\nu = \int dz P(z|\mathbf{m}) \tanh(\hat{\beta}(m_\nu + z)), \quad \nu = A + 1, \dots, P, \quad (135)$$

where $P(z|\mathbf{m})$ is the large N limit of $P_\mu(z|\{m_\rho, 1\})$ which was defined in (44), and only depends on the vector \mathbf{m} of basal activation.

For $P \ll N^\gamma$, we have $P(z|\mathbf{m}) \equiv \langle \delta(z - \sum_{\nu}^P \xi^\nu m_\nu) \rangle_{\boldsymbol{\xi}} \simeq \delta(z)$ and the equations decouple, hence there is no interference between infected and non-infected clones

$$m_\mu = \tanh(\hat{\beta}(m_\mu + \psi_\mu)), \quad \mu = 1, \dots, A, \quad (136)$$

$$m_\nu = \tanh(\hat{\beta}m_\nu), \quad \nu = A + 1, \dots, P. \quad (137)$$

For the infected clones, the presence of the field induces hysteresis effect in the clonal activation [23]. This may explain immunological memory effects [24, 12], without the requirement of dedicated memory cells: after an infection, the responsive B cells, may retain a non-zero activation as the antigen is fought and its concentration is sent to zero, and on a successive encounter with the same antigen they will provide a higher and faster response.

For $P = \mathcal{O}(N^\gamma)$, $P(z|\mathbf{m})$ in (134), (135), has a finite width, and both antigen-induced and basal activities reduce, due to clonal interference, and hysteresis cycles become smaller. However, the presence of antigens does not affect the basal activity of uninfected clones $\nu = A + 1, \dots, P$, as long as $A \ll N^\gamma$.

Next we investigate the scenario where the number of antigens is $A = \mathcal{O}(N^\gamma)$ and ask whether the system is able to fight against all of them in parallel. For simplicity, we set $P = N^\gamma$ and

$A = \phi_1 N^\gamma$, with ϕ_1 denoting the fraction of infected clones and we assume that all viruses have the same concentrations *i.e.* $\boldsymbol{\psi} = \psi(1, \dots, 1, 0, \dots, 0)$. This leads to the steady state equations

$$\begin{aligned} m_\mu &= \langle \tanh(\hat{\beta}(m_\mu + \psi + \sum_{\nu=1}^A (m_\nu + \psi)\xi^\nu + \sum_{\nu=A+1}^P m_\nu \xi^\nu)) \rangle_{\boldsymbol{\xi}} & \mu = 1, \dots, A \\ m_\nu &= \langle \tanh(\hat{\beta}(m_\nu + \sum_{\rho=1}^A (m_\rho + \psi)\xi^\rho + \sum_{\rho=A+1}^P m_\rho \xi^\rho)) \rangle_{\boldsymbol{\xi}} & \nu = A + 1, \dots, P \end{aligned} \quad (138)$$

Now antigen interference on the basal activity is relevant and will affect the activation of the non-infected clones. In the small field limit, we can Taylor expand (138) near $\hat{\beta} = 1 + \epsilon$ and small m_ν , obtaining

$$m_\mu \simeq (1 + \epsilon)m_\mu + \psi_\mu(1 + \epsilon) - \frac{1}{3} \left((m_\mu + \psi_\mu)^3 + \frac{3c}{N^\gamma} (m_\mu + \psi_\mu) \sum_{\rho \neq \mu} (m_\rho + \psi_\rho) \right) \quad (139)$$

For $\mu < A$ (infected clones) we have for $\psi \ll \epsilon$

$$m_\mu = \frac{-\psi(1 + \epsilon)}{\epsilon} \equiv m_1, \quad \mu = 1, \dots, A. \quad (140)$$

where the expansion holds for field $\psi \ll \epsilon$, otherwise $m_\mu = \mathcal{O}(1)$. For $\mu > A$ ($\psi_\mu = 0$) we have

$$m_\mu \simeq (1 + \epsilon)m_\mu - \frac{1}{3} \left(m_\mu^3 + \frac{3c}{N^\gamma} m_\mu \sum_{\rho \neq \mu} (m_\rho + \psi_\rho)^2 \right) \quad (141)$$

hence $m_\mu = 0$ is always a solution (uninfected clones may not be activated) together with

$$\begin{aligned} m_\mu^2 &= 3\epsilon - \frac{3c}{N^\gamma} \sum_{\rho} (m_\rho + \psi_\rho)^2 = \\ &= 3\epsilon - \frac{3c}{N^\gamma} \left(\sum_{\rho=A+1}^P m_\rho^2 + \sum_{\rho=1}^A (2m_1\psi + \psi^2) \right), \quad \mu = A + 1, \dots, P. \end{aligned} \quad (142)$$

This shows that uninfected clones are symmetrically activated, each one with intensity

$$m_2^2 = \frac{3\epsilon - 3c\phi_1\psi^2(2(1 + \epsilon)/\epsilon + 1)}{1 + 3c\phi_2} = \frac{3\epsilon(1 - 2c\phi_1(\frac{\psi}{\epsilon})^2)}{1 + 3c\phi_2}, \quad (143)$$

where $\phi_2 \leq 1 - \phi_1$ is the fraction of active uninfected clones. Hence, for $\psi \ll \epsilon$, clonal activation close to criticality will have the form $\mathbf{m}^* = (m_1, \dots, m_1, m_2, \dots, m_2, 0, \dots, 0)$. However, upon increasing the fraction ϕ_1 of infected clones or the antigenic field ψ , (143) shows that non-zero values of m_2 may become impossible and uninfected clones may get activated at a lower temperature (similarly to clones with smaller numbers of triggered receptors we dealt with in Sec. 4). This is confirmed by numerical results in Fig. 23, showing that the response of uninfected B clones and their activation temperature decrease for increasing fractions of infected clones. This results in a reduced basal activity of the immune system, which is vital to keep cells signaled and accomplish homeostasis [18]. In fig. 24 we study the impact of antigen concentration on

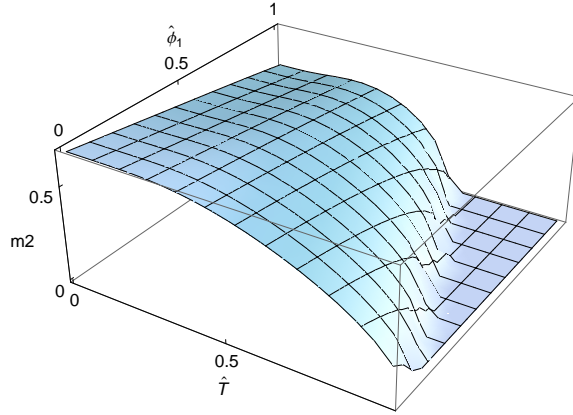


Figure 23. 3D plot of the activation m_2 of non-infected clones versus the fraction of infected clones $\hat{\phi}_1 = \phi_1 c$ and the scaled temperature $\hat{T} = T/c$, for fixed $\psi = 0.1$. Increasing $\hat{\phi}_1$ both the intensity and the critical activation temperature decrease, due to the antigenic interference.

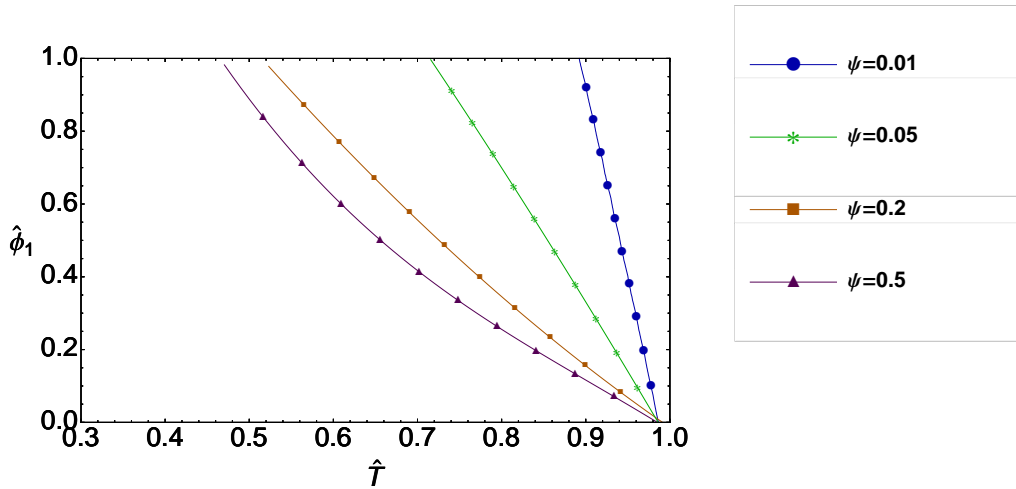


Figure 24. Critical line for the activation of uninfected clones in the space of scaled parameters $\hat{T} = T/c$, $\hat{\phi} = \phi c$, obtained from the condition $m_2 \neq 0$ (141), for different values of the antigenic field ψ . Increasing ψ , the region where uninfected clones are signaled shrinks.

the critical temperature at which uninfected B clones become responsive, by plotting the critical temperature versus the fraction of infected clones, for different values of antigen concentration. This shows that as the fraction of infected clones and the field increase, the basal activity is more and more compromised.

Next, we inspect the stability region of $\mathbf{m}^* = (m_1, \dots, m_1, m_2, \dots, m_2, 0, \dots, 0)$ by looking at the eigenvalues of the Jacobian of the dynamical system (131). This has a diagonal structure, in the thermodynamic limit, where off-diagonal elements become negligible and diagonal terms are

for $\mu < n_1 = \phi_1 N^\gamma$

$$J_{\mu\mu} = \hat{\beta}(1 - \langle \tanh^2(\hat{\beta}(m_\mu + \psi + \sum_{\nu=n_1+1}^{n_2} m_\nu \xi^\nu + \sum_{\nu=1}^{n_1} (m_\nu + \psi) \xi^\nu)) \rangle_{\boldsymbol{\xi}}) \quad (144)$$

for $n_1 < \mu < n_2 = \phi_2 N^\gamma$

$$J_{\mu\mu} = \hat{\beta}(1 - \langle \tanh^2(\hat{\beta}(m_\mu + \sum_{\nu=n_1+1}^{n_2} m_\nu \xi^\nu + \sum_{\nu=1}^{n_1} (m_\nu + \psi) \xi^\nu)) \rangle_{\boldsymbol{\xi}}) \quad (145)$$

and for $\mu > n_2$

$$J_{\mu\mu} = \hat{\beta}(1 - \langle \tanh^2(\hat{\beta}(\sum_{\nu=n_1+1}^{n_2} m_\nu \xi^\nu + \sum_{\nu=1}^{n_1} (m_\nu + \psi) \xi^\nu)) \rangle_{\boldsymbol{\xi}}) \quad (146)$$

Evaluating the Jacobian at the symmetric fixed point \mathbf{m}^* and introducing the distribution $P_n(z) = \langle \delta(z - \sum_{\nu=l}^{\ell+n} \xi^\nu) \rangle, \forall \ell$, gives

$$\lambda_1 = \hat{\beta} \left\{ 1 - \sum_{z_1, z_2} P_{n_1}(z_1) P_{n_2}(z_2) \tanh^2[\hat{\beta}((\psi + m_1)(1 + z_1) + m_2 z_2)] \right\} - 1 \quad \text{deg}(\lambda_1) = n_1 \quad (147)$$

$$\lambda_2 = \hat{\beta} \left\{ 1 - \sum_{z_1, z_2} P_{n_1}(z_1) P_{n_2}(z_2) \tanh^2[\hat{\beta}((\psi + m_1)z_1 + m_2(1 + z_2))] \right\} - 1 \quad \text{deg}(\lambda_2) = n_2 \quad (148)$$

$$\lambda_3 = \hat{\beta} \left\{ 1 - \sum_{z_1, z_2} P_{n_1}(z_1) P_{n_2}(z_2) \tanh^2[\hat{\beta}((\psi + m_1)z_1 + m_2 z_2)] \right\} - 1 \quad \text{deg}(\lambda_3) = P - n_1 - n_2 \quad (149)$$

with m_1, m_2 following from (140), (141) as

$$\begin{aligned} m_1 &= \sum_{z_1, z_2} P_{n_1}(z_1) P_{n_2}(z_2) \tanh[\hat{\beta}((\psi + m_1)(1 + z_1) + m_2 z_2)] \\ m_2 &= \sum_{z_1, z_2} P_{n_1}(z_1) P_{n_2}(z_2) \tanh[\hat{\beta}((\psi + m_1)z_1 + m_2(1 + z_2))] \end{aligned} \quad (150)$$

and $P_n(z) = e^{\phi c} I_z(\phi c)$ for $n = \phi N^\gamma$, where $I_z(x)$ is the modified Bessel function of the first kind. In Fig. 25 (left) we show the critical lines $\lambda_1 = 0$, $\lambda_2 = 0$ and $\lambda_3 = 0$ in the space of scaled parameters $\hat{T} = T/c$, $\hat{\phi}_2 = \phi_2 c$. As temperature is lowered, λ_3 is the first eigenvalue to destabilise, meaning that clonal activation will get in the form $\mathbf{m} = (m_1, \dots, m_1, m_2, \dots, m_2)$. Decreasing the temperature further, the system will first prioritise activation of infected clones, while keeping activation of uninfected clones symmetric, and later, at low temperature, will activate uninfected clones in a hierarchical fashion (see fig. 25, right panel). Near the critical temperature symmetric mixtures with $\phi_2 \leq 1 - \phi_1$ are stable. To investigate the optimal value of ϕ_2 we calculate the free-energy as a function of ϕ_2 for fixed T, ϕ_1

$$F(\phi_1, \phi_2) = -\frac{1}{\beta} \sum_{z_1, z_2} P_{n_1}(z_1) P_{n_2}(z_2) \log(2 \cosh(\beta c(m_1 + \psi)z_1 + m_2 z_2)) + \frac{c}{2}(\phi_1 m_1^2 + \phi_2 m_2^2) \quad (151)$$

which is minimal (fig. 26) at $\phi_2 = 1 - \phi_1$, meaning that the system will keep all uninfected clones signalled.

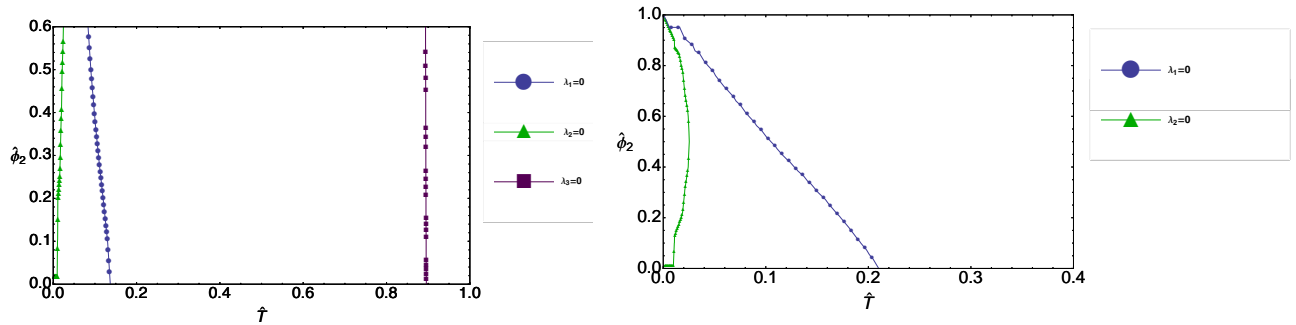


Figure 25. Left: Phase diagram in the space of scaled parameters $\hat{T} = T/c, \hat{\phi}_2 = \phi_2 c$ with $\phi_1 = 0.4$. Lines represent contours of $\lambda_1 = 0$ (circles), $\lambda_2 = 0$ (triangles) and $\lambda_3 = 0$ (squares). To the right of the line $\lambda_3 = 0$ solutions where uninfected clones are partially activated are stable. Lowering down the temperature and crossing the line $\lambda_1 = 0$ the m_1 symmetric mixtures destabilise, meaning that infected clones are hierarchically activated. Crossing the line $\lambda_2 = 0$ the m_2 symmetric mixtures destabilise, and uninfected clones are hierarchically activated. Right: Plots of $\lambda_1 = 0$ (circles), $\lambda_2 = 0$ (triangles) in the space $\hat{T} = T/c, \hat{\phi}_2 = \phi_2 c$ for $\phi_2 = 1 - \phi_1$.

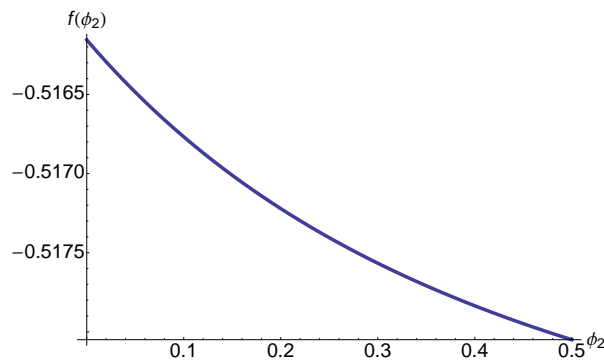


Figure 26. Free energy as a function of the fraction of active uninfected clones (ϕ_2) for $\phi_1 = 0.5$, $T = 0.7, c = 0.2, \psi = 0.05$.

7. Conclusions

In this paper we presented a minimal model for interacting cells in the adaptive immune systems, constituting of B cells, T cells and antigens. Our model is able to capture important collective features of the real immune system, such as the ability of simultaneously handling multiple infections, the dependence of B clones' activation on the number of receptors on clonal surface and the role of idiotypic interactions in enhancing parallel response to multiple infections. We analysed the dynamics of the system's order parameters quantifying the B clones' activation via linear stability analysis and Monte Carlo simulations. We found the regions, in the parameters' space, where the system activate B clones *symmetrically*, *i.e.* with the same intensity, or *hierarchically*, whereby the system prioritises responses to particular infections. We showed that clones with fewer receptors are less likely to be activated (Sec. 4) and idiotypic interactions contribute to the overall stability of the immune system, preventing unwanted activation and increasing the

region where *all clones* are equally activated and ready to start an immune response upon arrival of new infections (Sec. 5). Furthermore, we investigated how the immune system responds to antigens, showing in particular that multiple antigens create an interference that leads to less effective response to individual antigens and a reduction in the *basal activity* of the uninfected B cells (Sec. 6). For higher noise level the system tends to simultaneously fight *all* the antigens, despite losing in terms of response strength, whereas for lower noise level it will prioritise some infections over others. Finally, we showed that short term memory may emerge as an hysteresis effect, without the requirement of dedicated memory cells.

8. Acknowledgements

It is our great pleasure to thank ACC Coolen for many useful discussions.

References

- [1] Abbas A K, Lichtman A H, Pillai S, 2014 *Cellular and Molecular Immunology: with STUDENT CONSULT Online Access*. Elsevier Health Sciences.
- [2] Parisi G, 1990 *Proc. Natl. Acad. Sci. USA* **87** 429.
- [3] Weisbuch G, De Boer R J, Perelson A S, 1990 *Journal of theoretical biology* **146**(4) 483-499.
- [4] Mora T, Walczak A M, Bialek W, Callan Jr C G, 2010 *Proc. Natl. Acad. Sci. USA* **107** 5405.
- [5] Agliari E, Barra A, Bartolucci S, Galluzzi A, Guerra F and Moauro F, 2013 *Phys. Rev. E* **87** 042701.
- [6] Bartolucci S and Annibale A, 2014 *J. Phys. A: Math. Theor.* **47** 415001 doi:10.1088/1751-8113/47/41/415001
- [7] Kouskoff V, Lacaud G, Pape K, Retter M, Nemazee D, 2000 *Proc. Natl Acad. Sci. USA* Vol. **97** Issue 13.
- [8] Jerne N K, 1974 *Annales d'immunologie* **125C** (1-2) 373-389.
- [9] Menshikov I and Beduleva L, 2007 *International Immunology* Vol. **20** No. 2, pp. 193-198 doi:10.1093/intimm/dxm131
- [10] Pendergraft W F , Preston G A, Shah R R, Tropsha A, Carter C W, Jennette J C, Falk R J, 2004 *Nature medicine*, **10**(1) 72-79.
- [11] Shoenfeld Y, 2004 *Nature medicine* **10**(1) 17-18.
- [12] Janeway CA Jr, Travers P, Walport M, Shlomchik M, 2001 *Immunobiology: The Immune System in Health and Disease*. 5th edition. New York: Garland Science; Immunological memory. Available from: <http://www.ncbi.nlm.nih.gov/books/NBK27158/>
- [13] Hopfield J J, 1982 *Proc. Natl Acad. Sci. USA* **79** 2554-2558.
- [14] Amit D J, Gutfreund H and Sompolinsky H, 1985 *Phys. Rev. A* **32** 1007-1018.
- [15] Mezard M, Parisi G and Virasoro A ,1987 *Spin glass theory and beyond* (World Scientific, Singapore) .
- [16] Amit D J, 1989 *Modelling brain function*, Cambridge University Press.
- [17] Coolen ACC, Kuehn R and Sollich P, 2005 *Theory of neural information processing systems*, (Oxford University Press, Oxford).
- [18] E Agliari, A Annibale, A Barra, ACC Coolen, D Tantari, 2013, *J. Phys. A: Math. Theor.* **46** (41)
- [19] P Sollich, D Tantari, A Annibale, A Barra, 2014 *Phys. Rev. Lett.* **113** (23), 238106
- [20] Raff M, 1977 *Nature* **265**, 205 - 207 ; doi:10.1038/265205a0
- [21] Gao L, Zhou F, Li X, Jin Q, *PLoS One* **5** e10736 (2010)
- [22] Zonana-Nacach A, Camargo-Coronel A, Yanez P, Sánchez L, Jimenez-Balderas F J, Fraga A, 2001 *Lupus*, **10**(7) 505-510.
- [23] Kochmański M, Paszkiewicz T, Wolski S, 2013 *Eur. J. Phys.* **34** 1555 doi:10.1088/0143-0807/34/6/1555.
- [24] De Monvel, J H B and Martin O C, 1995 *Bulletin of mathematical biology* **57**(1) 109-136.

- [25] Viola A and Lanzavecchia A, 1996 *Science* Vol. **273**.
- [26] Abramowitz M and Stegun I A, 1972 *Handbook of Mathematical Functions*, (Dover, New York).
- [27] Laughton S N and Coolen A C C ,1995 *J. Stat. Phys.* **80** 1-2 375-387.